| AD NUMBER |
|---|
| AD912307 |
| LIMITATION CHANGES |

TO:

Approved for public release; distribution is unlimited. Document partially illegible.

FROM:

Distribution authorized to U.S. Gov't. agencies only; Test and Evaluation; JUL 1973. Other requests shall be referred to Naval Ship Research and Development Center, Code 11, Bethesda MD 20034.
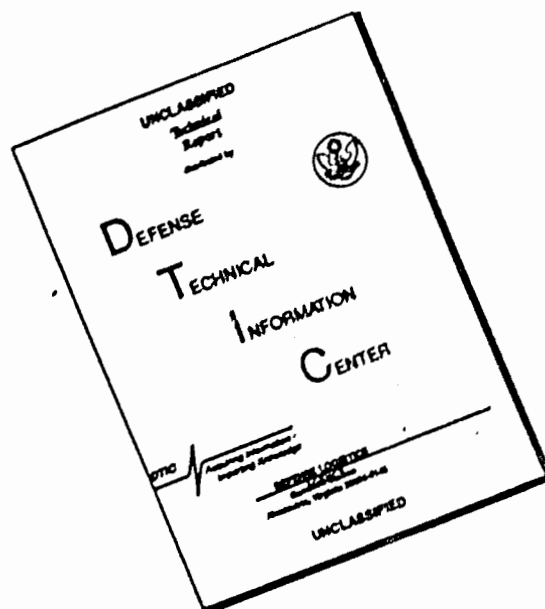
AUTHORITY

usnsrdc ltr, 27 aug 1976

THIS REPORT HAS BEEN DELIMITED
AND CLEARED FOR PUBLIC RELEASE
UNDER DOD DIRECTIVE 5200.20 AND
NO RESTRICTIONS ARE IMPOSED UPON
ITS USE AND DISCLOSURE.

DISTRIBUTION STATEMENT A

APPROVED FOR PUBLIC RELEASE;
DISTRIBUTION UNLIMITED.

# DISCLAIMER NOTICE

THIS DOCUMENT IS BEST QUALITY AVAILABLE. THE COPY FURNISHED TO DTIC CONTAINED A SIGNIFICANT NUMBER OF PAGES WHICH DO NOT REPRODUCE LEGIBLY.

# NAVAL SHIP RESEARCH AND DEVELOPMENT CENTER
Bethesda, Md. 20034

ARCTIC SURFACE EFFECT VEHICLE PROGRAM

PREDICTION OF AXIAL AND CENTRIFUGAL FAN
CHARACTERISTICS FOR LARGE SURFACE EFFECT VEHICLES

by
John G. Purnell

Sponsored by
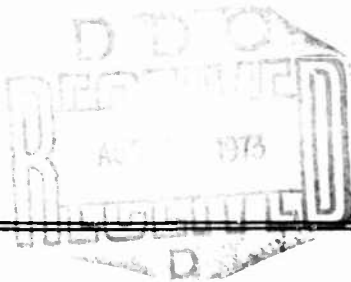
**PROPULSION AND AUXILIARY SYSTEMS DEPARTMENT**

Annapolis

**RESEARCH AND DEVELOPMENT REPORT**
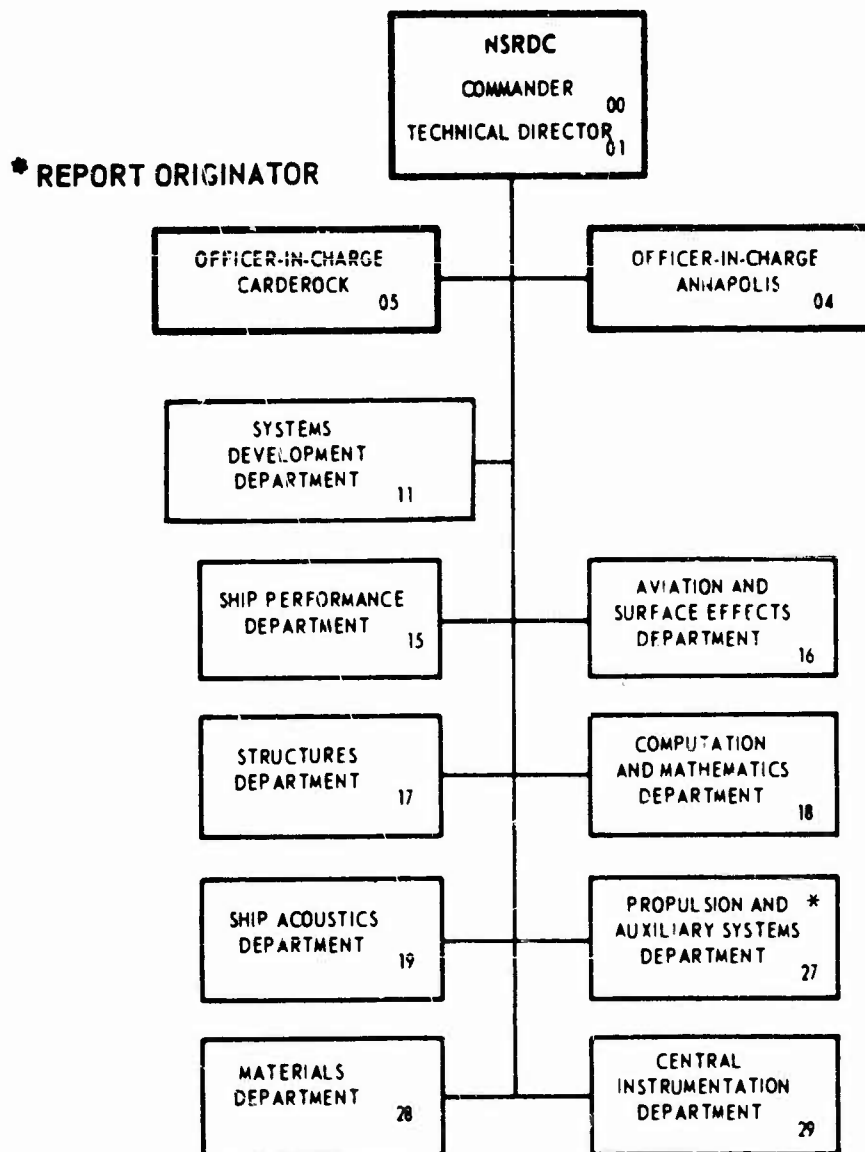
July 1973                                      Report 3943

The Naval Ship Research and Development Center is a U. S. Navy center for laboratory effort directed at achieving improved sea and air vehicles. It was formed in March 1967 by merging the David Taylor Model Basin at Carderock, Maryland with the Marine Engineering Laboratory at Annapolis, Maryland.

Naval Ship Research and Development Center

Bethesda, Md.   20034

## MAJOR NSRDC ORGANIZATIONAL COMPONENTS

```
                    ┌──────────────────────┐
                    │        NSRDC         │
                    │   COMMANDER     00   │
                    │ TECHNICAL DIRECTOR   │
                    │                 01   │
                    └──────────────────────┘
```

**\* REPORT ORIGINATOR**

```
┌──────────────────────┐          ┌──────────────────────┐
│  OFFICER-IN-CHARGE   │          │  OFFICER-IN-CHARGE   │
│    CARDEROCK         │          │    ANNAPOLIS         │
│              05      │          │              04      │
└──────────────────────┘          └──────────────────────┘

      ┌──────────────────────┐
      │      SYSTEMS         │
      │   DEVELOPMENT        │
      │   DEPARTMENT         │
      │              11      │
      └──────────────────────┘

┌──────────────────────┐          ┌──────────────────────┐
│  SHIP PERFORMANCE    │          │   AVIATION AND       │
│    DEPARTMENT        │          │  SURFACE EFFECTS     │
│              15      │          │   DEPARTMENT    16   │
└──────────────────────┘          └──────────────────────┘

┌──────────────────────┐          ┌──────────────────────┐
│   STRUCTURES         │          │   COMPUTATION        │
│   DEPARTMENT         │          │  AND MATHEMATICS     │
│              17      │          │   DEPARTMENT    18   │
└──────────────────────┘          └──────────────────────┘

┌──────────────────────┐          ┌──────────────────────┐
│  SHIP ACOUSTICS      │          │ PROPULSION AND  *    │
│   DEPARTMENT         │          │ AUXILIARY SYSTEMS    │
│              19      │          │   DEPARTMENT    27   │
└──────────────────────┘          └──────────────────────┘

┌──────────────────────┐          ┌──────────────────────┐
│   MATERIALS          │          │    CENTRAL           │
│   DEPARTMENT         │          │  INSTRUMENTATION     │
│              28      │          │   DEPARTMENT    29   │
└──────────────────────┘          └──────────────────────┘
```

# DEPARTMENT OF THE NAVY

# NAVAL SHIP RESEARCH AND DEVELOPMENT CENTER

BETHESDA, MD. 20034

## PREDICTION OF AXIAL AND CENTRIFUGAL FAN CHARACTERISTICS FOR LARGE SURFACE EFFECT VEHICLES

by
John G. Purnell

July 1973                    27-404                    Report 3943

## ABSTRACT

Two digital computer programs have been
formulated for predicting performance charac-
teristics of centrifugal and axial fans which
may be used to provide lift air for large sur-
face effect vehicles.  Pressure rise and flow
characteristics of forwardly curved, radial,
and backwardly curved centrifugal fans can be
evaluated.  Axial fans having either inlet
flow prerotators or exit flow straighteners
can also be handled in the program.  Sample
results are presented to illustrate the method
of calculation and the nature of the results.

## ADMINISTRATIVE INFORMATION

# TABLE OF CONTENTS

27-404

# NOMENCLATURE

## CENTRIFUGAL FAN (EQUATIONS 1 THROUGH 40)

### English

a   - Effective radius of interblade circulation, ft

A   - Area, ft²

b   - Blade height, ft

$C_d$ - Discharge coefficient

d   - Diameter, ft

e   - Characteristic roughness size, ft

g   - Acceleration of gravity, ft/sec²

$g_c$ - Gravitational constant, $lb_m$-ft/$lb_f$-sec²

k   - Loss coefficient

P   - Pressure, $lb_f$/ft²

$\Delta P$ - Pressure loss, $lb_f$/ft²

Q   - Volume flow, ft³/sec

r   - Radius, ft

$R_b$ - Blade height ratio, $b_1/b_2$

$R_d$ - Diameter ratio, $d_1/d_2$

U   - Impeller speed, ft/sec

V   - Velocity, ft/sec

w   - Weight flow, $lb_m$/sec

W   - Weight, $lb_m$

z   - Number of blades.

## Greek

$\beta$   - Blade angle (measured from tangent), degrees

$\beta_s$ - Preswirl angle, degrees

$\delta$   - Inlet clearance, ft

$\eta$   - Efficiency

$\rho$   - Density, $lb_m/ft^3$

$\Psi$   - Pressure coefficient

$\Delta\Psi$ - Pressure coefficient

$\emptyset$   - Flow coefficient

$\omega$   - Rotational speed, rad/sec.

## Subscripts and Superscripts

D     - Diffuser

e     - Inlet eye

E     - Modified Euler line

imp  - Impeller

in    - Inlet

leak - Leakage

m     - Radial condition

max  - Maximum

min  - Minimum

out   - Outlet

r     - Relative velocity

RC    - Recirculation loss

S     - Preswirl angle

static - Static conditions

total  - Total conditions

u     - Tangential velocity component

u'    - Corrected tangential velocity component

V     - Velocity pressure

0     - Impeller inlet

1     - Impeller blade inlet

2     - Impeller blade outlet

3     - Downstream of impeller outlet

∞     - Theoretical Euler line equation.


AXIAL FAN (EQUATIONS 41 THROUGH 95)

English

A   - Area, $ft^2$

c   - Blade chord, ft

$C_D$ - Drag coefficient

$C_L$ - Lift coefficient

D   - Diameter, ft

$g_c$ - Gravitational constant, $lb_m$-ft/$lb_f$-$sec^2$

j   - Number of blade sections

n   - Fan speed, rpm

N          - Number of blades

P          - Pressure, $lb_f/ft^2$

Q          - Airflow rate, $ft^3/sec$

r          - Radius, ft

s          - Blade pitch (spacing), ft

V          - Velocity, ft/sec

X          - Diameter ratio, $D_i/D_{tip}$

$C_L/C_D$     - Lift-to-drag ratio

$D_H/D_{tip}$ - Hub-to-tip ratio, $X_H = D_H/D_{tip}$ .

## Greek

$\alpha$   - Angle of attack, degrees

$\beta$   - Blade angle of impeller, degrees

$\gamma$   - Angle which relative velocity makes with the plane of rotation, degrees

$\delta$   - Angle which relative velocity makes with the axis of rotation, degrees

$\epsilon$   - Swirl coefficient

$\eta$   - Efficiency

$\theta$   - Camber angle, degrees

$\rho$   - Air density, $lb_m/ft^3$

$\sigma$   - Solidity, c/s

$\emptyset$   - Flow coefficient

$\Psi$   - Pressure coefficient

$\Delta\Psi$ - Pressure drop coefficient

$\omega r$ - Tangential velocity component, ft/sec.

## Subscripts and Superscripts

an    - Annulus

ax    - Axial direction

D     - Diffuser

des   - Design condition

duct - Duct

H     - Hub

i      - Blade section

imp   - Impeller

j      - Total number of blade sections

m     - Midspan of blade

o      - Zero lift condition

P     - Prerotator

PR    - Profile

S     - Straightener

sec   - Secondary

st    - Stall

T     - Total

th    - Theoretical

tip    - Blade tip

*      - Optimum condition

1     - Impeller inlet condition

2     - Impeller outlet condition.

# INTRODUCTION

Cushion air fan characteristics play an important part in the speed/range performance, as well as the riding quality of a surface effect vehicle (SEV). The most desirable fan characteristic is one having as flat a slope as possible, that is, a small change in pressure output for a large change in fan output flow rate at a given fan speed. The flatter the fan characteristic, the smoother the riding characteristics of the SEV.

At this time, only axial and centrifugal fans appear to have future application to large SEV craft.[1] This is due mainly to their high efficiencies but also to their low-to-moderate weight and size, and their proven feasibility and reliability. Centrifugal fans with backwardly curved blades have been used extensively in the relatively small SEVs that have been built to date. Axial fans have seen a very limited application on present SEVs, mainly due to the cost advantage of the simpler centrifugal fan, which may not be a decisive factor on larger craft.

In this report, digital computer programs are outlined for predicting fan characteristic curves for centrifugal and axial fans. One objective of these programs was to provide the fan performance prediction in a relatively uncomplicated manner so as to enhance their usefulness. A reasonably high accuracy can be achieved with the programs which mainly require only the geometric details of the fan to make the performance prediction. The centrifugal fan prediction program is based largely on the work of Osborne[2] and Shipway.[3] Additional modifications to account for nonuniform discharge velocities and recirculation losses were added. The centrifugal program will predict fan performance for a forwardly curved, radial, or backwardly curved centrifugal fan. The axial fan prediction program was the result of work presented by Wallis[4] and Shipway.[5] The axial program predicts performance for an axial fan having either exit flow straighteners or inlet flow prerotator using either isolated or cascade airfoil data.

With these programs, it is possible to predict the performance of a given axial or centrifugal fan with a reasonable degree of accuracy. Also, these programs will be used to study the effects of certain variables on the fan characteristic curve in order to determine what most significantly affects the fan characteristic slope.

---

[1]Superscripts refer to similarly numbered entries in the Technical References at the end of the text.

A printout of the present centrifugal and axial fan charac-
teristic prediction programs with sample data are shown in
appendixes A and B, respectively. Also, separate nomenclatures
are used for the axial and centrifugal fan, and no attempt has
been made to unify them since the similar expressions can have a
totally different form for the different fans. Appendix C pre-
sents the details of the centrifugal fan weight estimation proce-
dure.

PREDICTION OF CENTRIFUGAL FAN CHARACTERISTICS

The following method outlines a means of predicting centrif-
ugal fan characteristic curves for squirrel-cage-type fans which
are commonly used in SEVs. The prediction method follows similar
methods presented by Osborne[2] and Shipway[3] but several modifica-
tions have been made. These modifications include mainly a cor-
rection for nonuniform discharge velocities suggested in Shepherd[6]
and Wislicenus,[7] and a recirculation pressure loss proposed by
Galvas.[8] The characteristic pressure-flow curve is derived in
both dimensional and nondimensional form by considering the theo-
retical Euler line equation and substracting the various losses
from it. The method requires only the following fan geometry
and system parameters to predict results:

- Inlet and exit blade diameter.

- Inlet and exit blade heights.

- Inlet and exit blade angles.

- Inlet eye diameter.

- Number of blades.

- Exit flow area.

- Tip speed.

A comparison of predicted and experimental characteristics for a
HEBA/B-type centrifugal fan is made, and the effects of varying
this fan geometry on the characteristic curve is studied.

FLOW THROUGH THE CENTRIFUGAL FAN

By conservation of mass for steady incompressible flow, the
inlet flow to the fan will equal the flow out of the fan. How-
ever, the flow through the impeller is usually greater than the
inlet flow because of a leakage flow between the impeller and

casing which recirculates through the fan and is a function of the static pressure differential between the impeller inlet and outlet. Thus, referring to figure 1:

$$Q_{in} = Q_{out} \tag{1}$$

$$Q_{imp} = Q_{in} + Q_{leak} = Q_{out} + Q_{leak} \ . \tag{2}$$
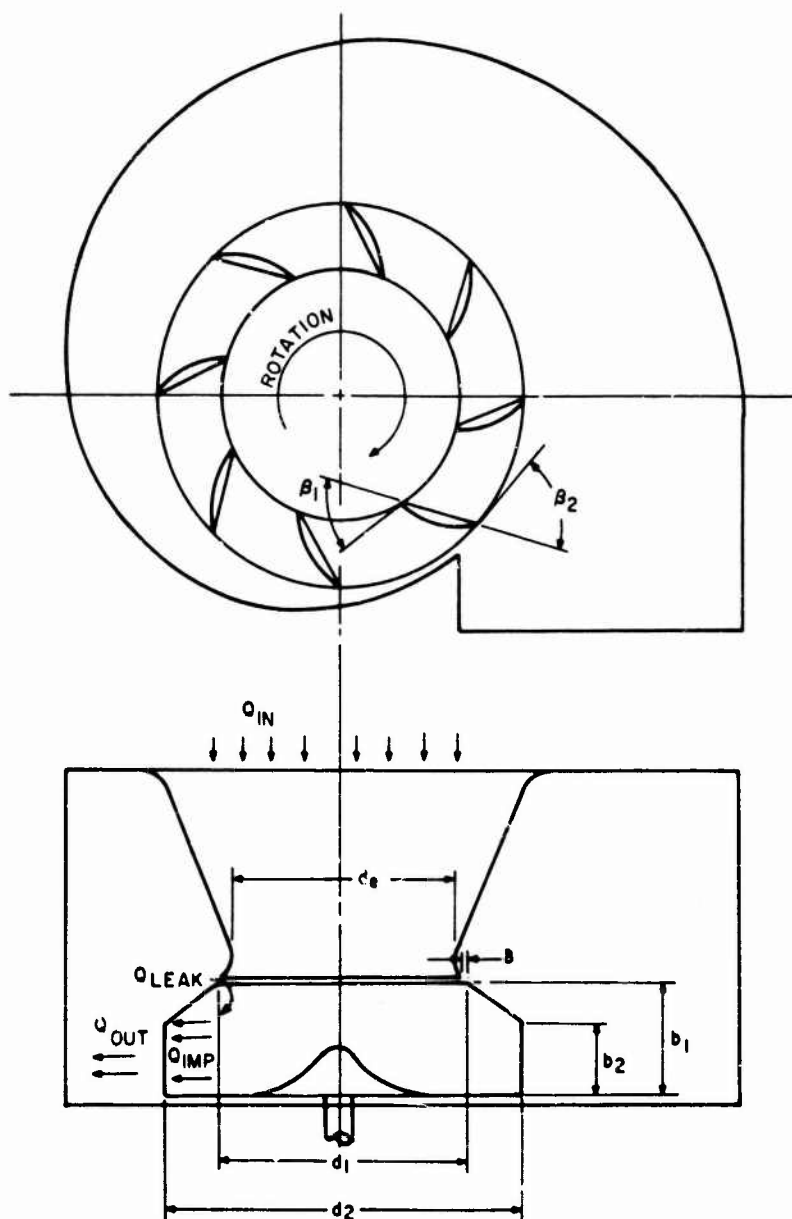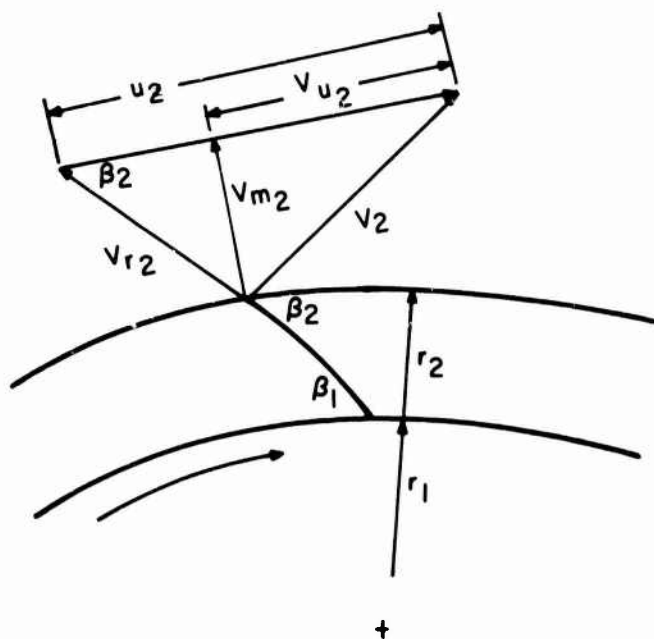


Figure 1
Geometry of a Centrifugal Fan

Therefore, in the analysis of the fan and its losses, the impeller should be based on equation (2) while the analysis of the inlet and outlet should be based on equation (1). It should be noted that even when $Q_{in}$ and $Q_{out}$ equal zero, $Q_{imp}$ can be greater than zero. The method of calculating $Q_{leak}$ will be shown later.

EULER LINE

The Euler line describes the maximum theoretical pressure flow line for the centrifugal fan. It considers the fan to have an infinite number of blades of infinitesimal thickness so that the entire airflow through the fan follows the blade contour exactly, thus producing the maximum pressure rise assuming no sources of loss are present. Figure 2 shows an outlet and inlet velocity diagram for a centrifugal fan impeller.

Item (a) - Outlet Velocity Diagram

Item (b)
Inlet Velocity Diagram
with Preswirl

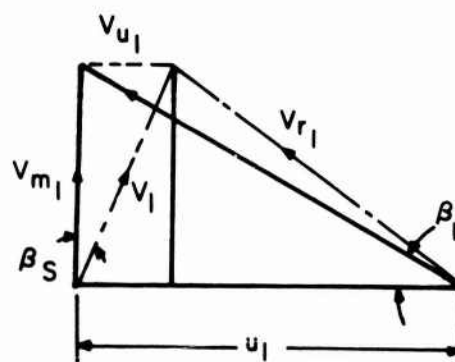FOR ZERO PRESWIRL $(\beta_S = 0)$

$V_{m_i} = V_I$



Figure 2
Centrifugal Fan Velocity Diagrams

In item (a) of figure 2, the tangential component of the absolute outlet velocity $V_2$ is $V_{u_2}$, while the radial component is $V_{m_2}$ and the relative velocity is $V_{r_2}$. The maximum work that can be done on the air will be equal to the energy in the air leaving the impeller, where, for radial inflow:

$$\text{maximum work} = P_\infty \, Q_{imp} = \frac{W}{g_c} \, V_{u_2} \, U_2 \, , \qquad (3)$$

where W is a weight flow rate of air. In terms of pressure rise rather than energy, equation (3) may be written as:

$$P_\infty = \frac{\rho}{g_c} \, V_{u_2} \, U_2 \; . \tag{4}$$

Using figure 1 and item (a) of figure 2, the following expression for $V_{u_2}$ is obtained:

$$V_{u_2} = U_2 - V_{m_2} \cot \beta_2$$

$$= U_2 - \frac{Q_{imp}}{\pi d_2 b_2} \cot \beta_2 \; , \tag{5a}$$

where

$$V_{m_2} = \frac{Q_{imp}}{\pi d_2 b_2} \; . \tag{5b}$$

Thus, the theoretical Euler line equation becomes

$$P_\infty = \frac{\rho}{g_c} U_2^2 - \frac{\rho \, U_2 \, Q_{imp}}{g_c \; \pi d_2 b_2} \cot \beta_2 \; . \tag{6}$$

The calculations carried out in terms of physical variables may be converted to dimensionless form by the use of two principal dimensionless variables:

$$\text{pressure coefficient} \quad \Psi = \frac{\text{pressure}}{\frac{\rho}{g_c} U_2^2} \; , \tag{7}$$

$$\text{flow coefficient} \quad \emptyset = \frac{\text{flow}}{d_2^2 \, U_2} \quad . \tag{8}$$

The pressure coefficient characterizes the dynamic condition of the flow and represents the pressure divided by the velocity pressure corresponding to the impeller tip velocity.[9] The flow coefficient expresses the kinematic conditions of the flow and represents the ratio of the axial velocity of the flow based on the fan diameter to the tip velocity of the fan impeller.[9] Hence, using the above expressions, equation (6) becomes (in nondimensional form):

$$\Psi_\infty = 1 - \emptyset_{imp} \frac{d_2}{\pi b_2} \cot \beta_2 \quad , \tag{9}$$

where $\emptyset_{imp}$ is based on $Q_{imp}$ of equation (2).

EFFECTS OF A FINITE NUMBER OF BLADES

The Euler line equation was derived by assuming the air exits the fan at exactly the trailing-edge blade angle. However, this is true only in the case of an infinite number of blades. This is particularly important for the impeller channel of a centrifugal machine where even for ideal flow (that is, without friction, turbulence, and separation), effects combine to modify the expression for the theoretical Euler line equation.

One cause of deviation of flow from the theoretical ideal is interblade circulation. Stodola[10] has suggested that it is the inertia effects of the fluid particles between adjacent blades of a radial flow impeller that must be considered. Due to their inertia, some particles tend to retain their orientation with respect to fixed axes, the result being a circulatory motion relative to the channel. This is similar to a container of fluid whirled with an angular velocity of $\omega$ at the end of an arm, as shown in figure 3, where a particle of fluid, A, tends to remain stationary. However, relative to a point on the container, B, point A appears to be rotating in a direction opposite but equal in magnitude to that of the arm. At any radius "a" within the container, the particle has a relative velocity of $-a\omega$.
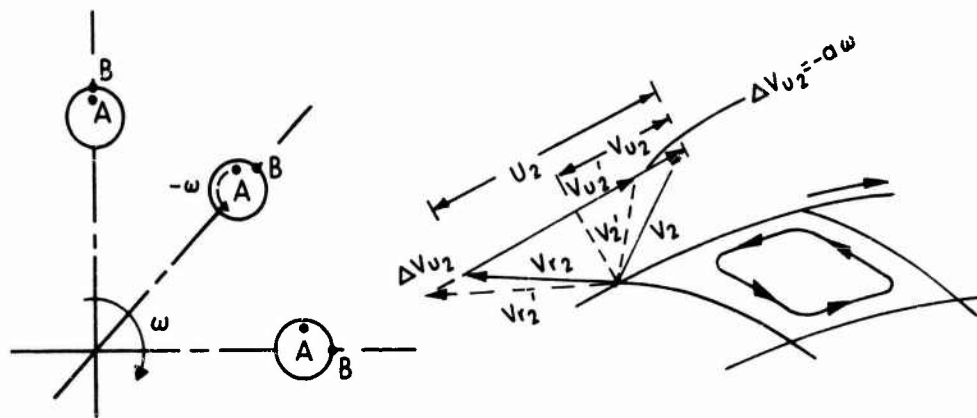
Figure 3
Interblade Circulation

Assuming that the impeller channel flow behaves similarly and that this motion is superimposed on the outward flow between the blades, the effect is to reduce the value of the tangential velocity $V_{u_2}$ to $V_{u_2}'$, where $V_{u_2}' = V_{u_2} - a\omega$. The effective radius of the area between the blades is difficult to assess, but is generally taken as half of the perpendicular distance between the blade tangents at the impeller periphery,[9] that is:

$$a = \frac{\pi d_2 \sin \beta_2}{2z} , \qquad (10)$$

where $z$ is the number of blades.

Since,

$$\omega = \frac{U_2}{r_2} = \frac{2U_2}{d_2}$$

$$a\omega = \frac{\pi d_2 \sin \beta_2}{2z} \cdot \frac{2U_2}{d_2} = \frac{\pi \sin \beta_2}{z} U_2 , \qquad (11)$$

and

$$V_{u_2}' = V_{u_2} - \frac{\pi \sin \beta_2}{z} U_2 \quad . \tag{12}$$

The net result of interblade circulation is to reduce the theoretical pressure based on the theoretical ideal velocity diagram. However, this reduction of output potential is the result of the behavior of an ideal fluid and does not represent a loss in terms of fluid and rotor energies because the impeller is not called upon to supply this additional energy. The significance of the interblade circulation correction is that by increasing the number of fan blades for a given fan, while maintaining constant tip speed, diameters, and blade angles, higher pressure outputs are possible since the flow more closely follows the blade profile angles; thus, the theoretical Euler line equation is more closely approached since interblade circulation effects are minimized.

The reduction in theoretical Euler pressure due to interblade circulation is expressed by:

$$\Delta P_b = \frac{\rho}{g_c} U_2 \; a\omega$$

$$= \frac{\rho}{g_c} U_2^2 \frac{\pi}{z} \sin \beta_2 \quad , \tag{13a}$$

and nondimensionally:

$$\Delta \Psi_b = \frac{\pi}{z} \sin \beta_2 \quad . \tag{13b}$$

EFFECTS OF NONUNIFORM DISCHARGE VELOCITY

Another effect which causes the fan to deviate from the theoretical Euler line is that the radial velocity may not be uniform along the discharge of the impeller. The pressure produced with a varying velocity is less than that produced with a uniform discharge velocity giving the same net flow rate. For a centrifugal fan having a linear variation of velocity across the depth of the channel, as shown in item (a) of figure 4, Shepherd[6] showed that:

$$\Delta P_{nd} = \frac{\rho \ U_2 \ Q_{imp}}{g_c \ \pi d_2 b_2} \left[ \frac{(V_{m_2}max - V_{m_2}min)^2}{12 \ V_{m_2}^2} \right] \cot \beta_2 \ , \qquad (14a)$$

and nondimensionally:

$$\Delta \Psi_{nd} = \frac{\emptyset_{imp} \ d_2}{\pi b_2} \left[ \frac{(V_{m_2}max - V_{m_2}min)^2}{12 \ V_{m_2}^2} \right] \cot \beta_2 \ . \qquad (14b)$$
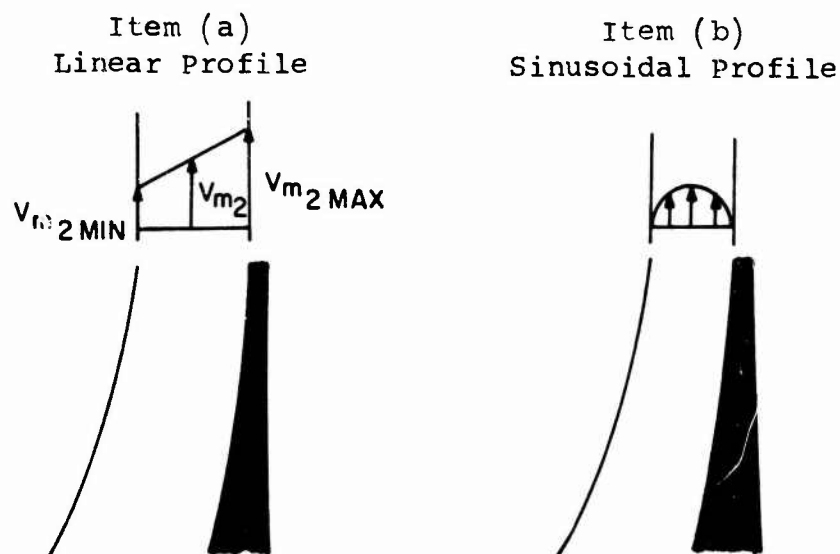
Item (a)
Linear Profile

Item (b)
Sinusoidal Profile



Figure 4
Nonuniform Discharge Velocity Distributions

For the case of a sinusoidal flow distribution, as shown in item (b) of figure 4, Wislicenus[7] showed that:

$$\Delta P_{nd} = \frac{\rho \ U_2 \ Q_{imp}}{g_c \ \pi d_2 b_2} \left[ \frac{\pi^2}{8} - 1 \right] \cot \beta_2 \ , \qquad (15a)$$

and nondimensionally:

$$\Delta\Psi_{nd} = \frac{\phi_{imp}\ d_2}{\pi b_2}\left[\frac{\pi^2}{8} - 1\right]\ \cot\ \beta_2\ . \qquad (15b)$$

Equations (15a) and (15b) also hold for a sinusoidal distribution in the peripheral direction around the impeller and the two velocity patterns may be superimposed giving a correction[7] factor of $[(\pi^2/8)^2 - 1]$. The causes of the nonuniform velocity distribution can be the manner in which the flow is turned from the axial to the radial direction in the inlet, as well as by real fluid effects such as friction and separation on the walls of the disk, shroud, and blades.

The net result of nonuniform discharge velocity is to reduce the maximum theoretical pressure predicted by the Euler line equation. However, like interblade circulation, this reduction in output potential does not represent a loss because the impeller is not called upon to supply this additional output. Radial velocity distributions at centrifugal fan outlets, shown by Brotherhood,[11] suggest that both linear and sinusoidal velocity distributions combined are generally present.

Although interblade circulation and nonuniform velocity distribution do not require or expend any energy, they do affect the fan efficiency since they represent lost potential which causes the theoretical Euler line to be modified downward. The modified Euler line equation on which efficiency is based now becomes:

$$P_E = P_\infty - \Delta P_b - \Delta P_{nd}\ , \qquad (16a)$$

and nondimensionally:

$$\Psi_E = \Psi_\infty - \Delta\Psi_b - \Delta\Psi_{nd}\ . \qquad (16b)$$

Thus, minimizing interblade circulation and nonuniform velocity distribution effects should improve efficiency, since the theoretical Euler line condition will be more closely approached.

27-404                          10

## IMPELLER LOSS

A loss occurs in the impeller due to separation of the fluid stream during flow through the blade passage and is defined as:

$$\Delta P_{imp} = k_{imp} \cdot \frac{1}{2} \frac{\rho}{g_c} (V_{r_1} - V_{r_2})^2 . \tag{17}$$

The value of $k_{imp}$ is between 0.2 and 0.3 for flat plate blades and on the order of 0.15 for aerofoil section blades.[2,3]

Zero preswirl has been assumed in the calculations of $V_1$ since $\Delta P_{imp}$ is very small at low flow rates and will not affect the final result, while at high flow rates preswirl is zero.[2,3] By considering the inlet and outlet velocity diagrams of figure 2 and putting,

$$V_{m_1} = \frac{Q_{imp}}{\pi d_1 b_1} \quad \text{and} \quad V_{m_2} = \frac{Q_{imp}}{\pi d_2 b_2} , \tag{18}$$

then equation (17) becomes:

$$\Delta P_{imp} = \frac{k_{imp}}{2} \frac{\rho}{g_c} Q_{imp}^2 \left[ \frac{1}{\pi d_1 b_1 \sin \beta_1} - \frac{1}{\pi d_2 b_2 \sin \beta_2} \right]^2 , \tag{19a}$$

and nondimensionally:

$$\Delta \Psi_{imp} = \frac{k_{imp}}{2} \left( \frac{\emptyset_{imp} d_2}{\pi b_2} \right)^2 \left[ \frac{1}{R_d R_b \sin \beta_1} - \frac{1}{\sin \beta_2} \right]^2 , \tag{19b}$$

where $R_d = d_1/d_2$ and $R_b = b_1/b_2$.

## INLET LOSSES

The inlet loss is divided into two parts.  First, air enters the impeller inlet section, usually through a reducing section, as shown in figure 1.  The airflow must expand from the velocity at the inlet eye, $V_e$, to the axial velocity, $V_o$, at the impeller inlet (or exit of the reducing section) and be turned from axial to radial flow.  The loss associated with the expansion may be expressed as:

$$\Delta P_{in_1} = \frac{k_{in_1}}{2} \frac{\rho}{g_c} V_e^2 \ . \tag{20}$$

Although the inlet conditions should be based on $Q_{in}$, the calculations may be simplified with minimal error by using $Q_{imp}$ since the leakage condition is not known until the outlet conditions are known.  Thus, equation (20) becomes:

$$\Delta P_{in_1} = \frac{k_{in_1}}{2} \frac{\rho}{g_c} \left[ \frac{4 \ast \ Q_{imp}}{\pi d_e^2} \right]^2 \ , \tag{21a}$$

and nondimensionally:

$$\Delta \Psi_{in_1} = \frac{k_{in_1}}{2} \emptyset_{imp}^2 \left[ \frac{4 \ d_2^2}{\pi d_e^2} \right]^2 \ . \tag{21b}$$

The value of $k_{in_1}$ ranges from 0.2 to 0.5.[2,3]

A second loss occurs as a result of expansion or contraction of the air as it enters the blade passages.  The loss also takes into account the effect of preswirl.  British work[3] suggests that for low flow rate where $V_o \leq V_{r_1}$, the preswirl angle, $\beta_s$, is on the order of 45 degrees.  At higher flow rates, where $V_o > V_{r_1}$, the preswirl angle is zero.  This loss is expressed by:

$$\Delta P_{in_2} = \frac{k_{in_2}}{2} \frac{\rho}{g_c} \left( V_o - V_{r_1} \right)^2 \ , \tag{22}$$

where $k_{in_2}$ lies between 0.5 and 0.8.[2,3] By substituting,

$$V_O = \frac{4^* \ Q_{imp}}{\pi d_1^2} \quad , \tag{23}$$

and from the inlet velocity diagram of item (b), figure 2,

$$V_{r_1} = \sqrt{V_{m_1}^2 + (U_1 - V_{m_1} \ \tan \ \beta_S)^2} \quad . \tag{24}$$

Thus, equation (22) becomes:

$$\Delta P_{in_2} = \frac{k_{in_2}}{2} \ \frac{\rho}{g_c} \left[ \frac{4 \ Q_{imp}}{\pi d_1^2} - \sqrt{V_{m_1}^2 + (U_1 - V_{m_1} \ \tan \ \beta_S)^2} \right]^2 \quad . \tag{25a}$$

In nondimensional form, this becomes:

$$\Delta \Psi_{in_2} = \frac{k_{in_2}}{2} \left[ \frac{4 \ \varnothing_{imp}}{R_d^2 \ \pi} \right.$$

$$\left. - \sqrt{\left( \frac{d_2 \ \varnothing_{imp}}{R_d R_b \ \pi b_2} \right)^2 (1 + \tan^2 \ \beta_S) - \frac{2d_2 \ \frac{\varnothing_{imp} \ \tan \ \beta_S}{\pi R_b b_2} + R_d^2}} \right]^2 \quad . \tag{25b}$$

The definitions of $R_d$, $R_b$, $\Delta \Psi$, and $\varnothing_{imp}$, equation (18), and various relationships obtained from the inlet velocity diagram (item (b), figure 2) must be substituted into equation (25a) in order to obtain equation (25b).

## LEAKAGE FLOW

Internal flow leakage occurs primarily between the impeller inlet and the casing inlet as shown in figure 1. Also, a leakage may occur around the drive shaft where it enters the casing, but this is far less serious than the inlet leakage and is not considered. The leakage volume that flows back into the inlet from the impeller exit area may be treated as flow through an orifice, that is, the leakage volume may be written:

$$Q_{leak} = C_d \, \pi d_1 \, \delta \sqrt{\frac{2P_{static} \, g_c}{\rho}} \, , \qquad (26a)$$

where $C_d$ is a discharge coefficient on the order of 0.6,[3] $P_{static}$ is the static pressure increase across the fan impeller, and $\delta$ is the clearance between impeller and casing. Written nondimensionally:

$$\phi_{leak} = C_d \, \frac{d_1}{d_2^2} \, \pi \, \delta \sqrt{2\psi_{static}} \, , \qquad (26b)$$

where $\psi_{static} = P_{static}/(\rho/g_c) \, U_2^2$. In general, the static pressure difference ($P_s$) is nearly equal to the fan total pressure ($P_{total}$), due to the static depression caused by the inlet velocity pressure and, thus, $P_{total}$ may be used in place of $P_{static}$ without significant error.

For the case of $Q_{out} = 0$, a static pressure difference exists across the fan impeller. Thus, a leakage flow exists, and there is a flow through the impeller, $Q_{imp} = Q_{leak}$, even though the flow downstream is zero.

## RECIRCULATION LOSS

The recirculation pressure loss is due to the leakage flow reentering the intake and causing additional work to be done to overcome dissipation, turning, and mixing losses. Osborne[2] and Shipway[3] do not consider a recirculation loss, although Galvas[8] does consider a somewhat similar loss. The recirculation loss appeared to be best expressed as a function of the leakage flow velocity where:

$$\Delta P_{RC} = k_{leak} \cdot \frac{1}{2} \frac{\rho}{g_c} \left( \frac{Q_{leak}}{\pi d_1 \delta} \right)^2 , \qquad (27)$$

where $k_{leak}$ appears to lie between 0.2 and 0.5 based on recalculating data presented by Shipway[3] used to compare to experimental data. Substituting equation (26a) in (27) yields:

$$\Delta P_{RC} = k_{leak} C_d^2 P_{static} , \qquad (28a)$$

and nondimensionally:

$$\Delta \Psi_{RC} = k_{leak} C_d^2 \Psi_{static} . \qquad (28b)$$

OUTLET LOSSES

There is almost always an increase of flow area from the blade passage to the volute casing which may range up to 2 1/2 times. Thus, there is a tendency for retardation of flow velocity with resultant eddy formation. This is expressed as an expansion-type loss by:

$$\Delta P_{out} = k_{out} \frac{1}{2} \frac{\rho}{g_c} [V_2' - V_3]^2 . \qquad (29)$$

The coefficient $k_{out}$ will vary with deviation from design conditions, but at maximum efficiency it is probably on the order of 0.4.[2,3] Also,

$$V_3 = \frac{Q_{out}}{A_3} \qquad (30)$$

where $V_3$ is the average velocity at some measuring station of area, $A_3$, which may be at the volute casing exit. If $V_3$ is measured close to the fan outlet, the case where $V_3 = V_2'$ is obtained, and hence $\Delta P_{out} = 0$. From the outlet velocity diagrams, item (a) of figure 2 and figure 3, the following is obtained:

$$V_2' = \sqrt{\left(U_2 - \frac{Q_{imp}}{\pi d_2 b_2} \cot \beta_2 - \frac{U_2 \pi}{z} \sin \beta_2\right)^2 + \left(\frac{Q_{imp}}{\pi d_2 b_2}\right)^2} \quad . \quad (31)$$

Written nondimensionally, equation (29) becomes:

$$\Delta\Psi_{out} = \frac{k_{out}}{2}\left[\left(\left(1 - \frac{\phi_{imp}\, d_2}{\pi b_2} \cot \beta_2 - \frac{\pi}{z} \sin \beta_2\right)^2 + \left(\frac{\phi_{imp}\, d_2}{\pi b_2}\right)^2\right)^{1/2} - \frac{\phi_{out}\, d_2^2}{A_3}\right]^2 . \quad (32)$$

In many present SEV installations, the centrifugal fan is mounted directly in a large plenum rather than a volute. No attempt is made to recover the tangential component of velocity, such as by mounting exit turning vanes. In this case, the outlet pressure loss is due entirely to the dissipation of the tangential component of velocity[12] and is stated as:

$$\Delta P_{out} = \frac{\rho}{g_c} \frac{V_{u_2}'^2}{2} \quad , \quad (33a)$$

or nondimensionally:

$$\Delta\Psi_{out} = \frac{1}{2}\left(\frac{V_{u_2}'}{U_2}\right)^2 , \quad (33b)$$

where $V_{u_2}'$ is obtained from equation (12).

EFFICIENCY

The efficiency of a fan is generally defined as the ratio of useful output power to the required input power to the impeller. The input power to the impeller is equal to the product of the impeller volume flow rate and the modified Euler line pressure of equations (17) or (18). Thus,

$$\text{input power} = Q_{imp}{}^* \, P_E \, , \qquad (34a)$$

or nondimensionally,

$$\text{input power} = \emptyset_{imp}{}^* \, \Psi_E \, . \qquad (34b)$$

The outlet power is equal to the product of the outlet pressure times the outlet volume flow rate. The outlet volume flow rate is equal to the impeller volume flow rate minus the leakage flow rate, which flows back toward the fan inlet and is calculated from equations (26a) or (26b). The outlet pressure may be based on either the total or static pressure conditions. The total pressure condition is obtained from:

$$P_{total} = P_E - \Delta P_{imp} - \Delta P_{in_1} - \Delta P_{in_2} - \Delta P_{RC} - \Delta P_{out} \, , \qquad (35a)$$

and nondimensionally:

$$\Psi_{total} = \Psi_E - \Delta \Psi_{imp} - \Delta \Psi_{in_1} - \Delta \Psi_{in_2} - \Delta \Psi_{RC} - \Delta \Psi_{out} \, . \qquad (35b)$$

The static pressure condition is obtained from:

$$P_{static} = P_{total} - \Delta P_v \, , \qquad (36a)$$

or

$$\Psi_{static} = \Psi_{total} - \Delta \Psi_v \, , \qquad (36b)$$

where $\Delta P_V$ and $\Delta \Psi_V$ represent velocity pressure and

$$\Delta P_V = \frac{1}{2} \frac{\rho}{g_c} V_2'^2 \qquad \text{(if static and total pressure are measured at fan exit),}$$

(37a)

or

$$\Delta P_V = \frac{1}{2} \frac{\rho}{g_c} V_3^2 \qquad \text{(if static and total pressure are measured downstream of fan);}$$

(37b)

and nondimensionally:

$$\Delta \Psi_V = \frac{1}{2} \left( \frac{V_2'}{u_2} \right)^2 \qquad \text{(if static and total pressure are measured at fan exit),}$$

(38a)

or

$$\Delta \Psi_V = \frac{1}{2} \left( \frac{V_3}{u_2} \right)^2 \qquad \text{(if static and total pressure are measured downstream of fan).}$$

(38b)

The fan total efficiency may now be expressed as:

$$\eta_{total} = \frac{P_{total}}{P_E} \cdot \frac{Q_{imp} - Q_{leak}}{Q_{imp}} = \frac{\Psi_{total}}{\Psi_E} \cdot \frac{\emptyset_{imp} - \emptyset_{leak}}{\emptyset_{imp}} \ .$$

(39a)

The static efficiency is expressed by:

$$\eta_{static} = \frac{P_{static}}{P_E} \cdot \frac{Q_{imp} - Q_{leak}}{Q_{imp}} = \frac{\Psi_{static}}{\Psi_E} \cdot \frac{\emptyset_{imp} - \emptyset_{leak}}{\emptyset_{imp}} \ .$$

(39b)

The efficiency of an impeller and volute (or diffuser) will
always be less than that of just the impeller. The difference
will be determined by the efficiency of the volute, $\eta_D$, where

$$\eta_D = \frac{P_E - \Delta P_{out}}{P_E} = \frac{\Psi_E - \Delta \Psi_{out}}{\Psi_E} \quad . \tag{40}$$

In some cases, fan characteristics which are presented by manu-
facturers are based on measurements at the exit of the fan
diffuser or volute. However, efficiencies quoted with these
fan characteristics often do not include the outlet loss and
represent only the higher fan impeller efficiency. Thus, when
comparing experimental and predicted data it is important to
know how the experimental data were obtained.

COMPARISON OF EXPERIMENTAL AND PREDICTED RESULTS

The fan characteristic prediction program was used to pre-
dict experimental performance for a 60-inch outside diameter (OD)
backwardly-curved, airfoil-bladed, HEBA/B centrifugal fan. The
results are shown in figure 5 along with all the losses. Agree-
ment between experimental and predicted value is quite good, but
this depends to some extent on the selection of loss coefficients
which requires either experience or experimental background to
make proper selections. For the present case, the following loss
coefficients were used:

$$k_{imp} = 0.15$$

$$k_{in_1} = 0.28$$

$$k_{in_2} = 0.7$$

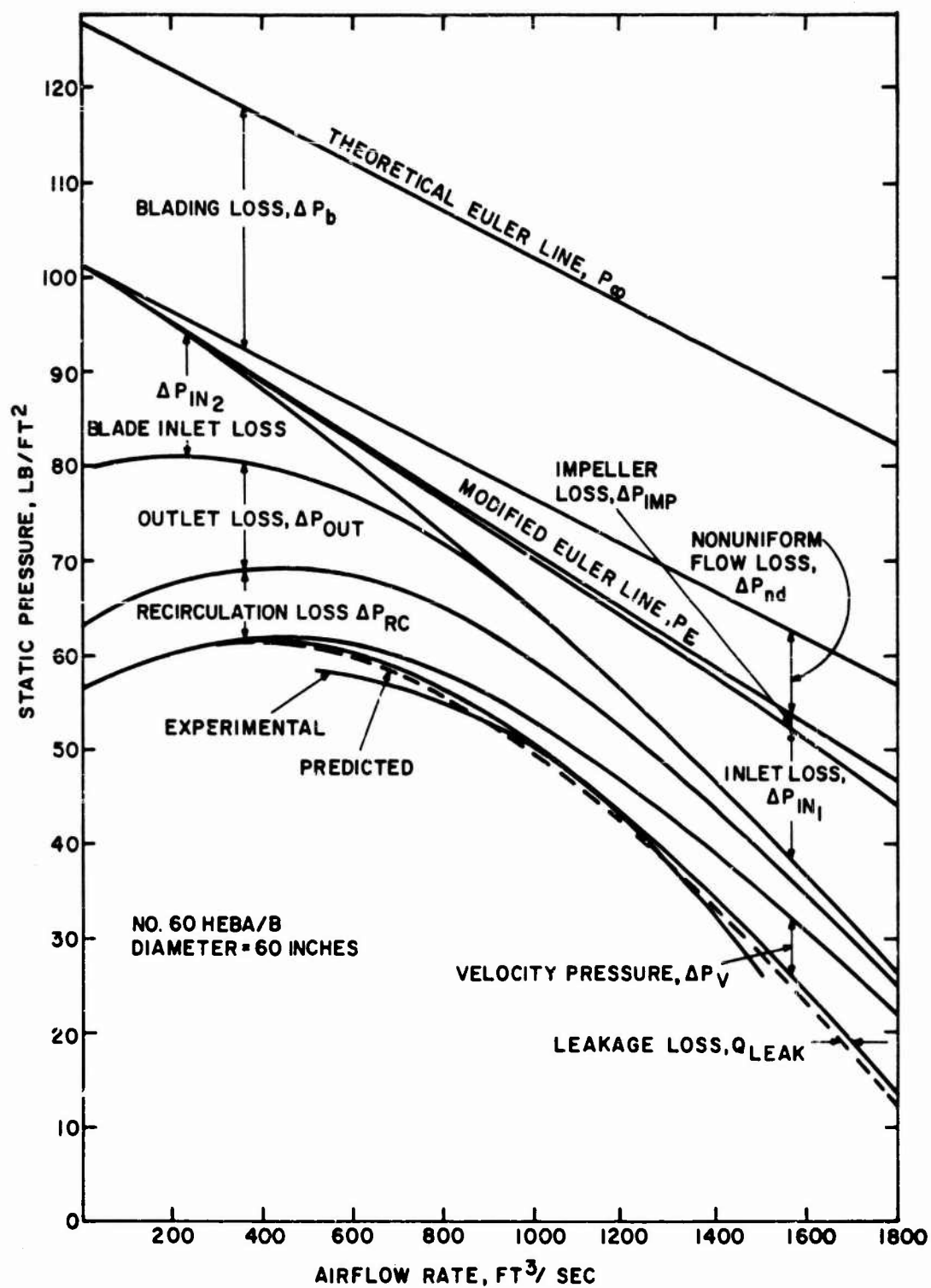$$k_{leak} = 0.3$$

$$k_{out} = 0.4.$$

Figure 5
Comparison of Predicted and Experimental Results

Also, the following physical variables describe the HEBA/B centrifugal fan system:

$$V_{tip} = 233 \text{ ft/s}^\dagger$$

$$d_1 = 3.46 \text{ ft}$$

$$d_2 = 5.00 \text{ ft}$$

$$b_1 = 1.62 \text{ ft}$$

$$b_2 = 1.18 \text{ ft}$$

$$\beta_1 = 25 \text{ degrees}$$

$$\beta_2 = 50 \text{ degrees}$$

$$z = 12 \text{ blades}$$

$$A_3 = 21 \text{ ft}^2 \text{ (volute exit)}$$

$$d_e = 0.9 * d_1$$

$$C_d = 0.6$$

$$\delta = 1/16 \text{ inch per foot of inside diameter (ID).}$$

A sinusoidal nonuniform discharge velocity is assumed to be occurring at the impeller outlet since this helps simplify the calculations and does not appear to offer any significant error in results over assuming a linear profile or combination.

Of particular interest for SEVs is having a fan with as flat a characteristic as possible, that is, having a large change of flow rate for a small pressure change at a given fan speed. To see what effect the different variables have on the fan characteristic curve, most of the above variables for the HEBA/B centrifugal fan were varied above and below the actual values in the prediction program. Items (a) through (h) of figure 6 show the results where one variable at a time was varied with the resultant static pressure and efficiency being plotted against the outlet airflow rate.

---

†Abbreviations used in this text are from the GPO Style Manual, 1973, unless otherwise noted.

Item (a)
Effects of Inside Diameter
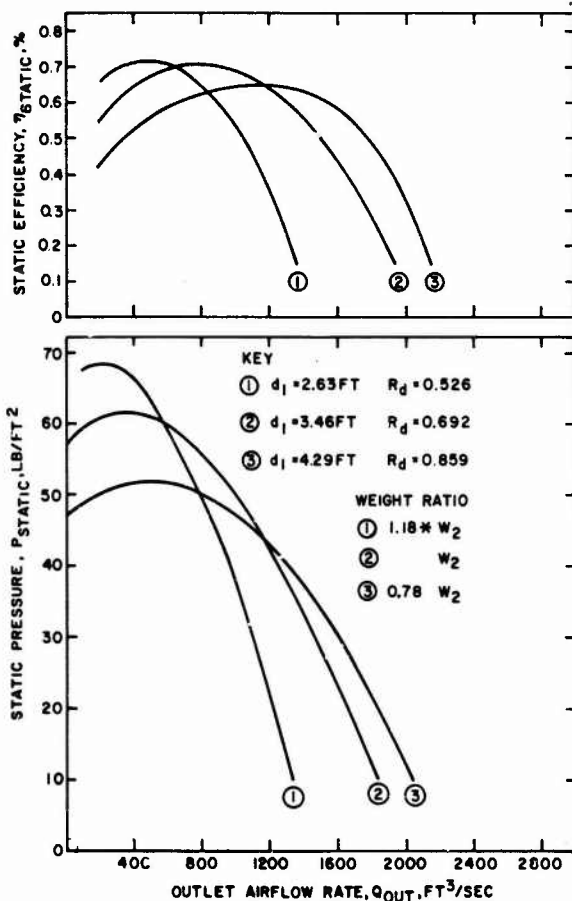
Item (b)
Effects of Outside Diameter
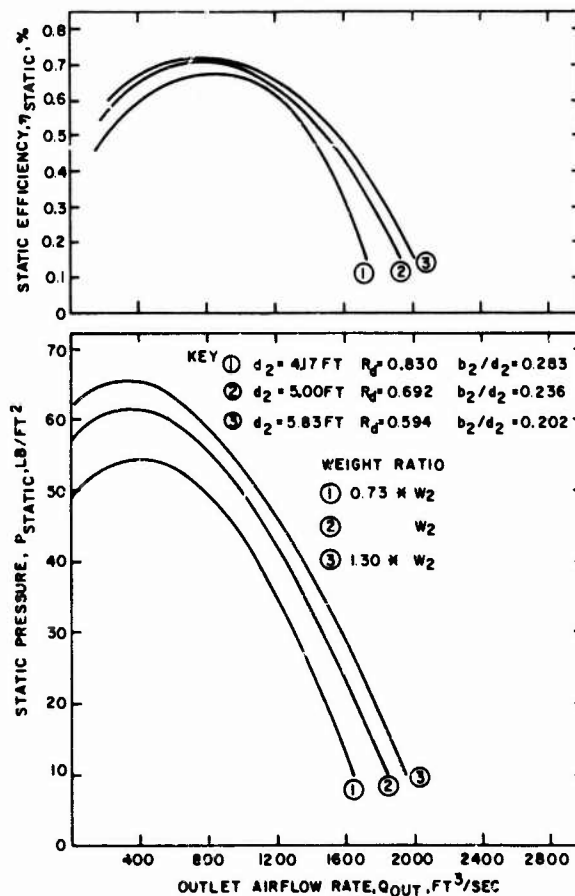
Figure 6
Effects of Centrifugal Fan Parameters

Item (c)
Effects of Inside
Blade Height
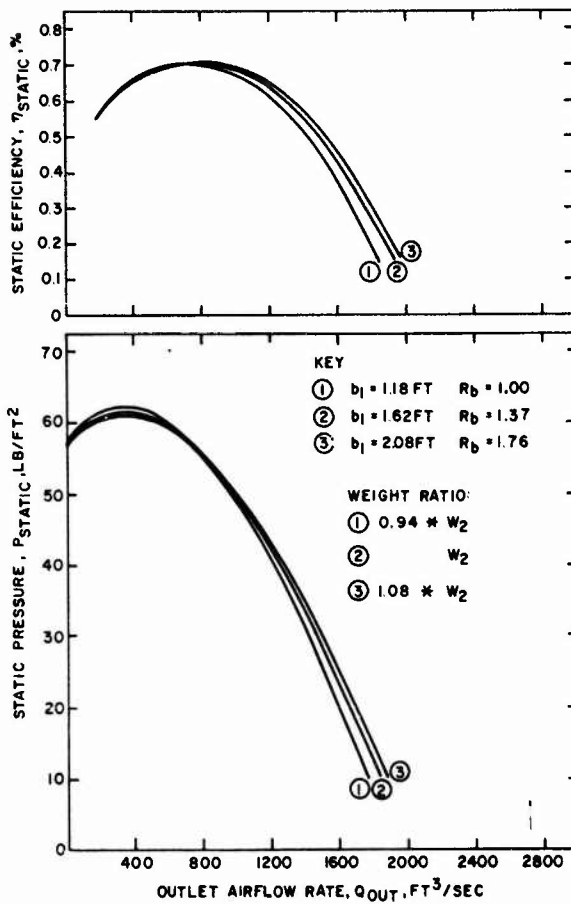
Item (d)
Effects of Outside
Blade Height

Figure 6 (Cont)

23

STATIC EFFICIENCY, $\eta_{STATIC}$, %

STATIC PRESSURE, $P_{STATIC}$, LB/FT$^2$

KEY
① $\beta_1 = 20°$
② $\beta_1 = 25°$
③ $\beta_1 = 30°$

WEIGHT RATIO
① 1.02 * $W_2$
② $W_2$
③ 0.98 * $W_2$

OUTLET AIRFLOW RATE, $Q_{OUT}$, FT$^3$/SEC
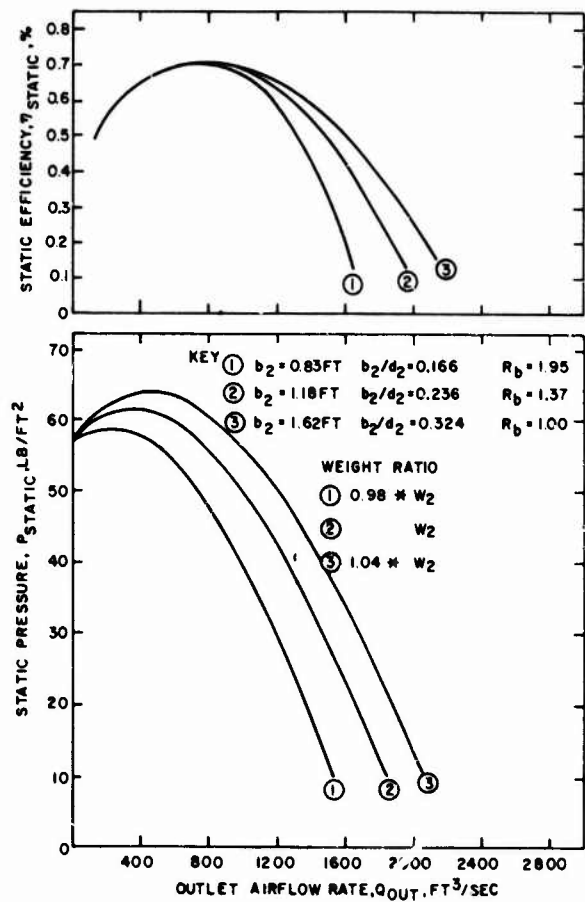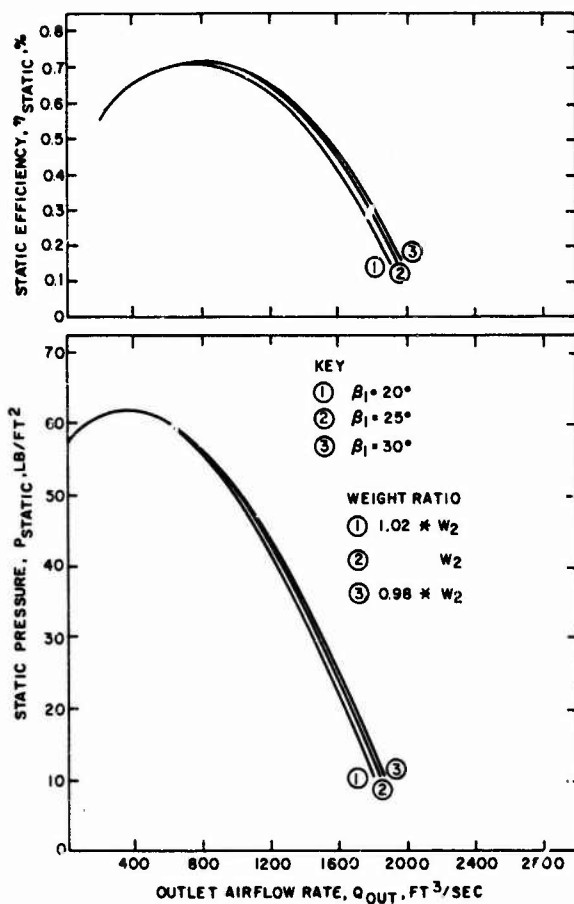
Item (e)
Effects of Inlet
Blade Angle

STATIC EFFICIENCY, $\eta_{STATIC}$, %

STATIC PRESSURE, $P_{STATIC}$, LB/FT$^2$

KEY
① $\beta_2 = 40°$
② $\beta_2 = 50°$
③ $\beta_2 = 60°$

WEIGHT RATIO
① 1.04 * $W_2$
② $W_2$
③ 0.97 * $W_2$

OUTLET AIRFLOW RATE, $Q_{OUT}$, FT$^3$/SEC

Item (f)
Effects of Exit
Blade Angle

Figure 6 (Cont)

Item (g)
Effect of Number
of Blades

Item (h)
Effects of Outlet Area

Figure 6 (Cont)

Included in the figures is an estimate of how the variable change affects basic fan impeller and hub weight as compared to the original HEBA/B fan noted 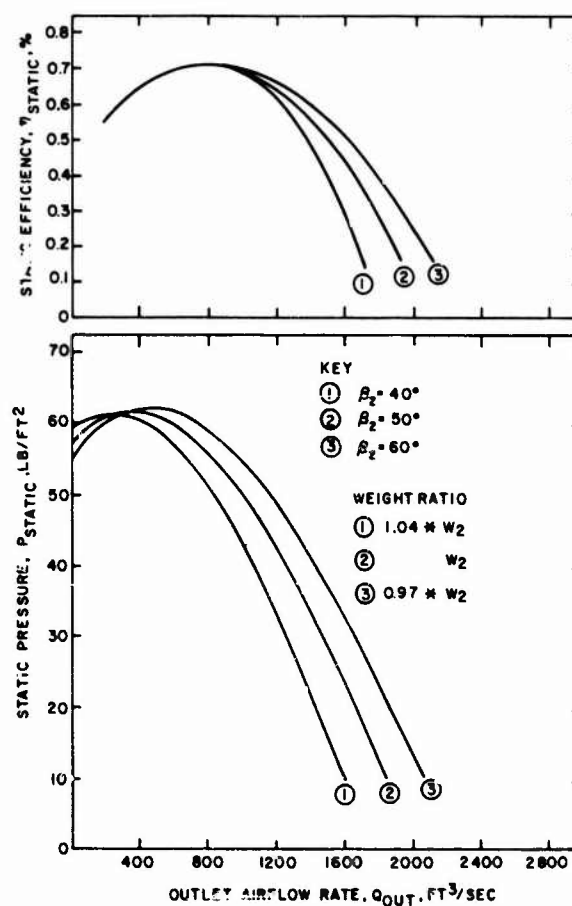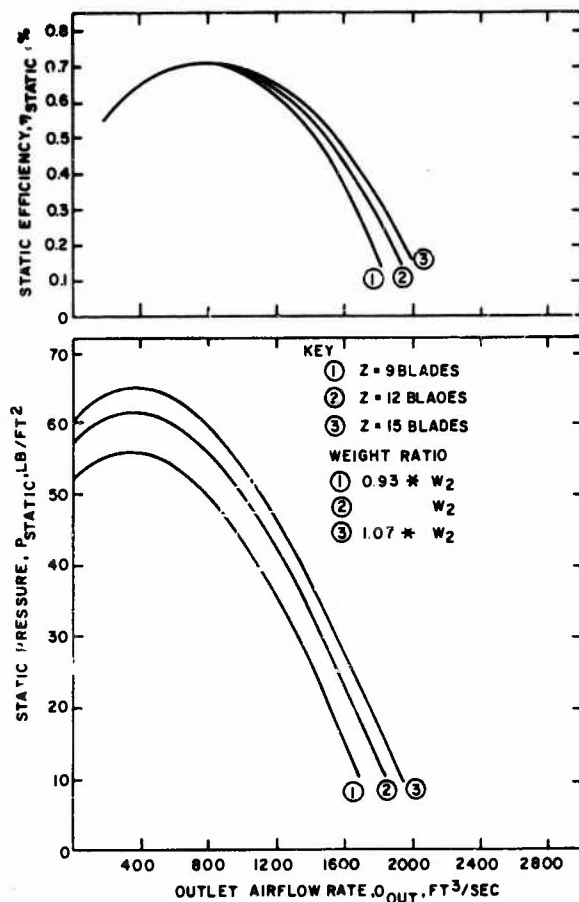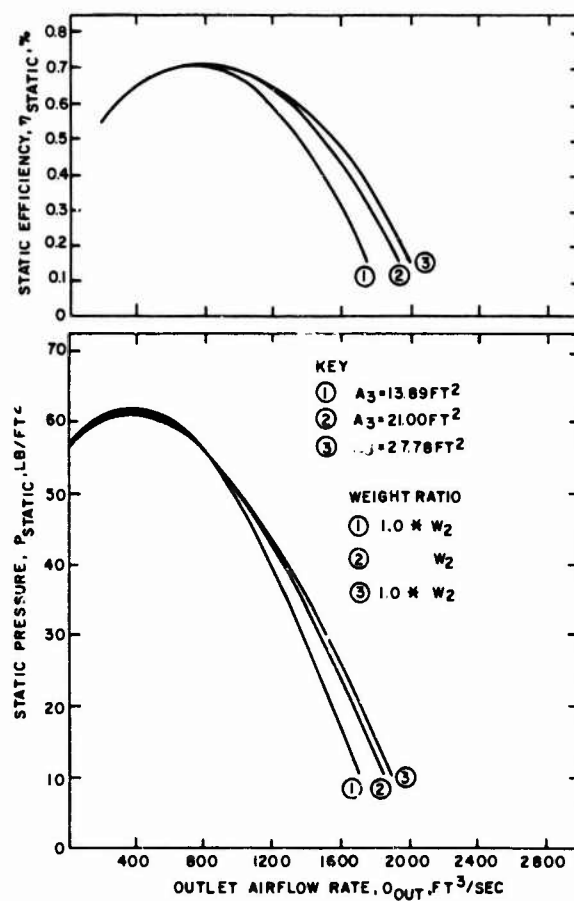as curve 2 in all figures. The rational for the weight estimates is shown in appendix C. Item (a) of figure 6 showed the most significant effect on characteristic slope. When the fan inside diameter approached the outside diameter, a significantly flatter characteristic resulted, although peak efficiency was reduced compared to the original fan. The fan static efficiency and pressure are both determined at the fan volute exit. Variation of the other parameters in items (b) through (h) did not significantly affect the slope or peak efficiency but could affect the pressure flow output. In figure 7, both the inlet and exit blade heights were changed together. Increasing the fan blade height allows greater airflow through the fan at a slightly increased pressure and a slightly more favorable slope without significantly affecting peak efficiency.

Figure 7
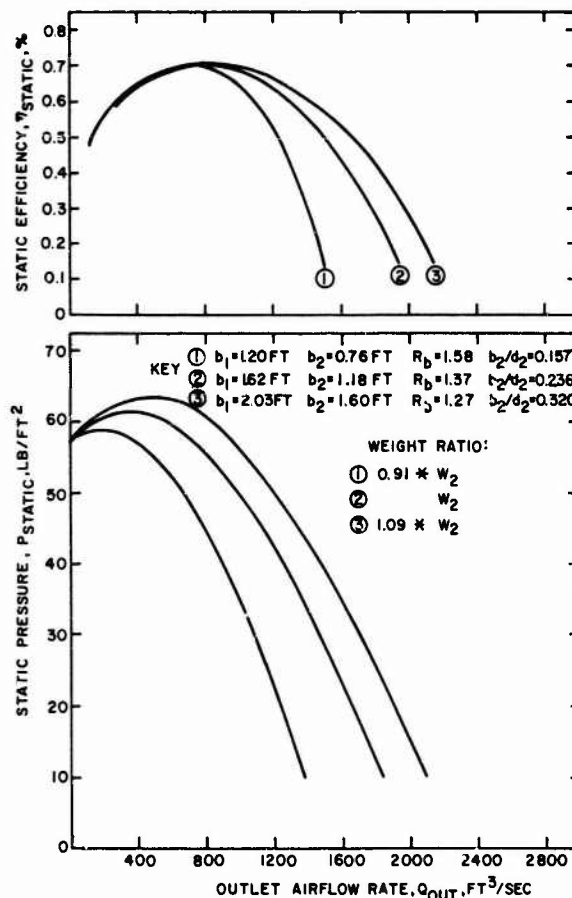Effects of Changing
Blade Height

LIMITATIONS ON CENTRIFUGAL FAN PREDICTION PROGRAM

It has been found that size affects efficiency when geometrically similar fans of different size are compared.[13] Increasing the fan diameter for a family of similar fans will cause the fan efficiency to increase due to a decrease in relative roughness ($e/d$), where $e$ = characteristic roughness size. The

characteristic roughness remains more or less constant in manu-
facturing processes so that relative roughness (e/d) varies
inversely as the fan diameter. The degree of modification for
size effects is small compared to the accuracy limits of the
above method and has been omitted to simplify the calculations.

Increasing the number of fan blades in the above program
has the effect of improving output flow and pressure as well as
efficiency, since interblade circulation effects are minimized
to provide a higher modified Euler line. To avoid designs having
too many or too few blades, the pitch-to-chord ratio of the fan
is generally maintained between 0.5 and 1.5.[14]

## AXIAL FAN CHARACTERISTICS PREDICTION

The method of predicting axial flow lift fan characteristic
curves was based on work by Wallis[4] and Shipway.[5] Using this
method, axial fans could be designed with either prerotator or
straightener vanes, as is usual with surface effect vehicles.
The program requires the basic geometry of the fan and the
characteristics of the desired airfoil blade to be used. Both
isolated airfoil and cascade data can be used in the program,
depending on the solidity value calculated for the fan.

The method for predicting axial fan characteristics is
essentially divided into three sections:

- Preliminary design

- Detailed design

- Off-design characteristics.

In the preliminary design, the fan efficiency and other variables
based on given flow, pressure, and geometry are estimated. The
detail design will specify the geometric details, such as inlet
and exit angles of the fan blade and the prerotator or straight-
ener blades. The off-design characteristics predict the varia-
tion of fan pressure and efficiency with flow rate for a given
fan speed.

PRELIMINARY DESIGN

The preliminary design is necessary to calculate and estimate some of the variables that will be needed in the later detailed design. The preliminary design estimates the total fan efficiency based on the following input design variables:

- Total pressure, $P_{T_{des}}$

- Flow, $Q_{des}$

- Outside (or tip) diameter, $D_{tip}$

- Inside (or hub) diameter, $D_H$, or hub-to-tip ratio, $X_H$

- Tip speed, $V_{tip}$, or fan r/min, n.

Various combinations of the above variables can be tried at this point to determine the optimum fan design dictated normally by the highest efficiency. At the end of the preliminary design, the basic physical dimensions have been determined and a more refined design will be performed to detail the aerodynamic design of the fan.

The preliminary design procedure requires the five input variables above and proceeds to calculate total fan efficiency for a fan having one of two options:

- Prerotators (or inlet guide vanes)

- Straighteners (or exit guide vanes).

If prerotators are used, the case is denoted by having the straightener swirl coefficient equal to zero ($\epsilon_s = 0$). If straighteners are used, then the prerotator swirl coefficient is zero ($\epsilon_p = 0$). The swirl coefficient represents the ratio of the tangential velocity component to the axial velocity component at a given radius. The design method used does not cover the case of using both prerotators and straighteners at the same time.

The axial velocity through the fan for a given flow is calculated by:

$$V_{ax} = \frac{Q}{\pi \frac{D_{tip}^2}{4}(1 - X_H^2)} \quad , \tag{41}$$

where $X_H = D_H/D_{tip}$. The flow coefficient at the blade tip is determined by:

$$\emptyset_{tip} = \frac{Q}{D_{tip}^2 V_{tip}} \quad , \tag{42a}$$

at the hub,

$$\emptyset_H = \frac{\emptyset_{tip}}{X_H} \quad , \tag{42b}$$

and at the midspan of the blade,

$$\emptyset_m' = \frac{\emptyset_{tip}}{\left(\frac{D_H + D_{tip}}{2 D_{tip}}\right)} = \frac{2 \emptyset_{tip}}{1 + X_H} \quad . \tag{42c}$$

The conditions at the tip, hub, and midspan of the blade, in general, represent the extremes and average conditions associated with the fan. Thus, conditions at these three sections are important and each is required to be known to assure a proper axial fan design.

The theoretical total pressure coefficient is calculated in dimensionless terms by:

$$\psi_{th} = \frac{P_T}{\frac{\rho}{g_c} V_{tip}^2} \quad . \tag{43}$$

For the fan design, it has been assumed that the total pressure rise and the axial velocity component remains constant along the blade length and that there is no radial component of flow. These assumptions fulfill the requirement for the free vortex flow that the fan design is based on.

The impeller swirl coefficient, which is defined as the ratio of the tangential-to-axial velocity component, is obtained from:[4],[5]

$$\epsilon_{imp_{tip}} = \frac{4\ V_{tip}^2}{\pi\ V_{ax}^2\ \eta_T\ (1 - X_H^2)}\ \Psi_{th}\ \emptyset_{tip}\ , \tag{44a}$$

$$\epsilon_{imp_m} = \epsilon_{imp_{tip}} \cdot \frac{2}{(1 + X_H)}\ , \tag{44b}$$

$$\epsilon_{imp_H} = \frac{\epsilon_{imp_{tip}}}{X_H}\ , \tag{44c}$$

where $\eta_T$ is the total fan efficiency and is assumed to be 0.8 for initial calculations. The swirl coefficient is an important variable in that it represents a measure of the torque of the impeller, in this case, and will be used in many subsequent equations.

The product of lift coefficient ($C_L$) and solidity ($\sigma = C/S$) at a section on the blade is given by:[4]

$$(C_L\sigma) = 2\ \epsilon_{imp}\ \sin\ \gamma_{imp}\ , \tag{45}$$

where $\gamma_{imp}$ is the angle between the resultant velocity through the fan impeller and the plane of rotation and is expressed by:[4]

$$\gamma_{imp} = \tan^{-1}\left(\frac{4\phi}{\pi(1 - X_H^2) - 2\,\epsilon_{imp}\,\phi}\right) \quad \begin{array}{l} \text{(if straighteners} \\ \text{are used, } \epsilon_p = 0)\,, \end{array}$$

$$\tag{46a}$$

or

$$\gamma_{imp} = \tan^{-1}\left(\frac{4\phi}{\pi(1 - X_H^2) + 2\,\epsilon_{imp}\,\phi}\right) \quad \begin{array}{l} \text{(if prerotators} \\ \text{are used, } \epsilon_s = 0)\,. \end{array}$$

$$\tag{46b}$$

Figures 8 and 9 show the geometric and velocity vector details of the blades which are used for the above and following equations. If equation (45) is to be solved at the hub, the appropriate values of $\phi_H$, $\epsilon_{imp_H}$, and $\gamma_{imp_H}$ at the hub must be used in the equations. Likewise, if the value at the midspan is desired, the values of $\phi_m$, $\epsilon_{imp_m}$, and $\gamma_{imp_m}$ must be used. In equations to follow, the subscript 'H' means values at the hub and the subscript 'm' means values at the midspan.

AXIS OF
ROTATION

$\theta$ = CAMBER ANGLE

$\sigma = \dfrac{C}{S}$
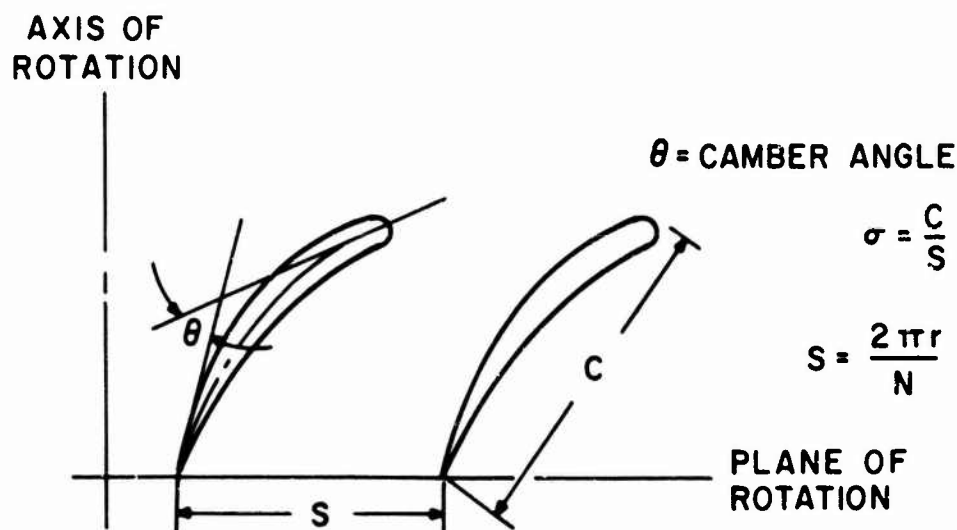
$S = \dfrac{2\pi r}{N}$

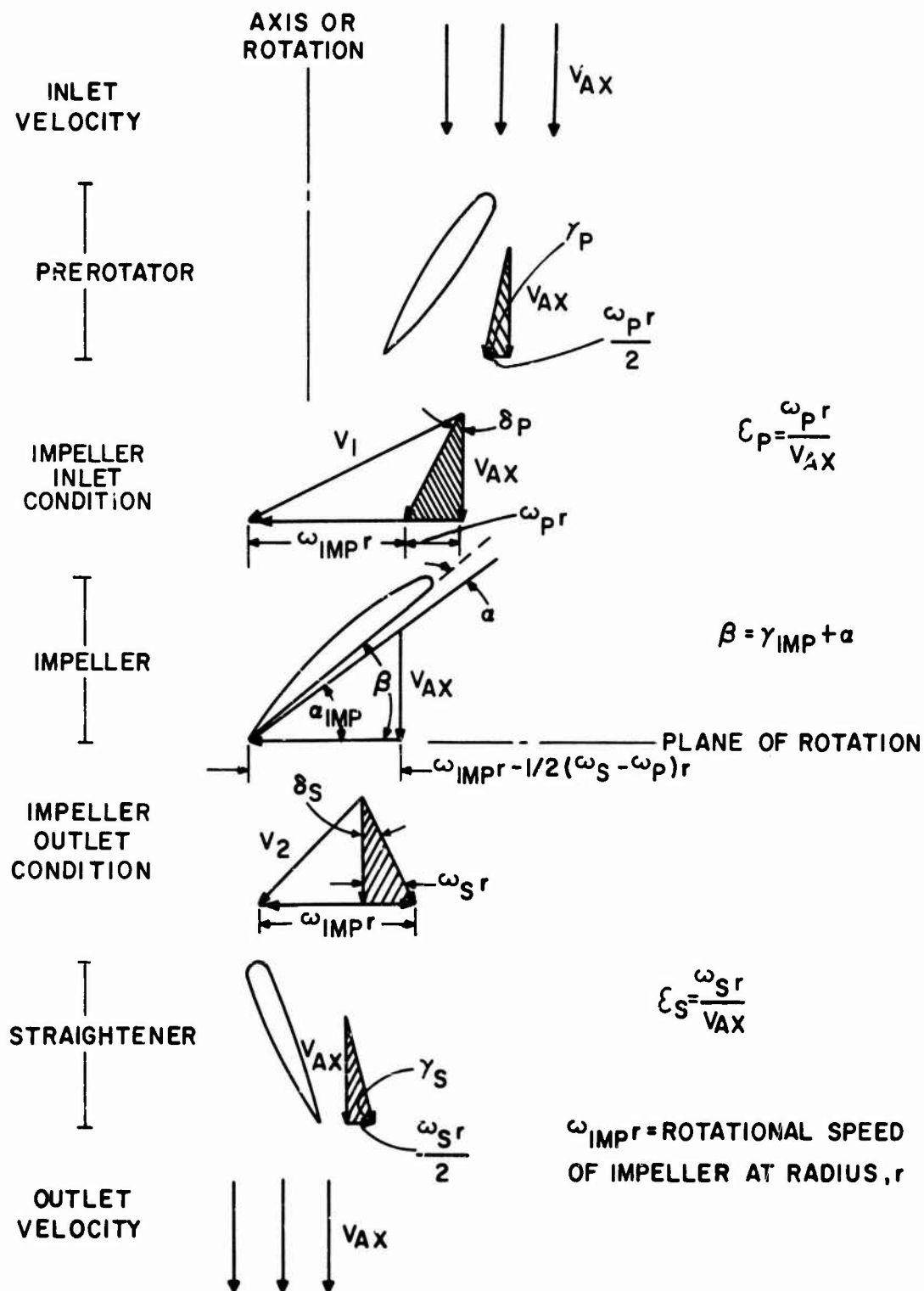PLANE OF
ROTATION



Figure 8
Geometric Details of Blades

Figure 9
Velocity Vectors for Fan System

With increasing static pressure rise across the fan impeller, there is a sharp increase in drag just prior to blade stalling. Maximum efficiency or optimum conditions should occur just before this rapid increase occurs. The following relationships[4] express the optimum lift coefficient $(C_L^*)$:

$$C_L^* = 2 \left[ \frac{1 + \left( \dfrac{\pi(1 - X_H^2)}{4\emptyset} \right)^2}{1 + \left( \dfrac{\pi(1 - X_H^2) + 4\, \epsilon_{imp}\, \emptyset}{4\emptyset} \right)^2} \right]^{1.375} \quad (\text{if } \epsilon_s = 0),$$

(47a)

or

$$C_L^* = 2 \left[ \frac{1 + \left( \dfrac{\pi(1 - X_H^2) - 4\, \epsilon_{imp}\, \emptyset}{4\emptyset} \right)^2}{1 + \left( \dfrac{\pi(1 - X_H^2)}{4\emptyset} \right)^2} \right]^{1.375} \quad (\text{if } \epsilon_p = 0).$$

(47b)

The solidity at any blade section may then be obtained by dividing equation (45) by (47). Thus,

$$\sigma = \left( \frac{C_L \sigma}{C_L^*} \right).$$

(48)

The value of $\sigma$ at the blade hub should be checked to assure that it is within the design limits of $\sigma_H \leq 1.5$. If $\sigma_H$ exceeds 1.5, the preliminary design input variables should be changed (i.e., increasing $V_{tip}$ and/or $X_H$ will decrease $\sigma_H$) and the calculations up to this point repeated.

The profile, secondary, and annulus losses associated with the impeller can now be calculated. The values are obtained at the midspan of the blade since they should represent the mean

loss for the impeller as a whole. The loss of efficiency due to profile drag[4,5] is:

$$\frac{\Delta\Psi imp_{PR}}{\Psi_{th}} = \frac{C_{D_{PR}}}{C_L} \cdot \frac{\phi}{\sin^2 \gamma_{imp}} \cdot \frac{4}{\pi(1 - X_H^2)} \quad , \tag{49}$$

where $\gamma_{imp}$ is obtained from equation (46) and $C_{D_{PR}}$ is the profile drag coefficient. The loss of efficiency due to secondary losses is obtained by:[4,5]

$$\frac{\Delta\Psi imp_{sec}}{\Psi_{th}} = \frac{C_{D_{sec}}}{C_L} \cdot \frac{\phi}{\sin^2 \gamma_{imp}} \cdot \frac{4}{\pi(1 - X_H^2)} \quad , \tag{50}$$

where $C_{D_{sec}}$ is the secondary drag coefficient. Combining equations (49) and (50) yields:

$$\frac{\Delta\Psi imp_{PR} + \Delta\Psi imp_{sec}}{\Psi_{th}} = \frac{C_{D_{PR}} + C_{D_{sec}}}{C_L} \cdot \frac{\phi}{\sin^2 \gamma_{imp}} \cdot \frac{4}{\pi(1 - X_H^2)} \quad . \tag{51}$$

Shipway[5] suggests that for this case the value of lift-to-drag ratio can be set as constant for preliminary evaluation as,

$$\frac{C_L}{C_{D_{PR}} + C_{D_{sec}}} = 20.5 \quad . \tag{52}$$

The magnitude of the annulus drag loss was assumed by Wallis[4] not to vary greatly from fan to fan and hence he suggests:

$$\frac{\Delta^{\Psi}imp_{an}}{\Psi_{th}} = 0.02 \quad \text{(for aerofoil-shaped blades)}$$

$$= 0.03 \quad \text{(for constant thickness plate blades)}. \tag{53}$$

The fan impeller efficiency can then be determined by adding equations (51) and (53) or,

$$\eta_{imp} = \frac{\Delta^{\Psi}imp_{PR}}{\Psi_{th}} + \frac{\Delta^{\Psi}imp_{sec}}{\Psi_{th}} + \frac{\Delta^{\Psi}imp_{an}}{\Psi_{th}} \quad . \tag{54}$$

The loss in efficiency caused by prerotator or straightener vane pressure drop must be determined. If straighteners only are used,[4]

$$\epsilon_s = \epsilon_{imp} \quad \text{and} \quad \epsilon_p = 0 , \tag{55}$$

and also[4]

$$\frac{\Delta^{\Psi}_s}{\Psi_{th}} = \frac{c_{D_s}{}^* \; \emptyset}{(2.18 - 1.43 \, \epsilon_s) \, \sin^2 \gamma_s} \cdot \frac{4}{\pi(1 - X_H^2)} \quad \text{(for } 0.5 \leq \epsilon_s < 1.0\text{)}, \tag{56a}$$

or[4]

$$\frac{\Delta^{\Psi}_s}{\Psi_{th}} = \frac{c_{DS}{}^* \; \emptyset}{3 \, \epsilon_s \, \sin^3 \gamma_s} \cdot \frac{4}{\pi(1 - X_H^2)} \quad \text{(for } \epsilon_s < 0.5\text{)}, \tag{56b}$$

where

$$\gamma_s = \cot^{-1}\left(\frac{\epsilon_s}{2}\right) \quad . \tag{57}$$

The straightener and prerotator pressure loss are both calculated at the midspan of the blade. $C_{D_S}$ is the straightener drag coefficient. It is made up of the sum of the profile and secondary drag coefficients for the straightener blade. Wallis[4] recommends the following drag coefficients be used:

$$C_{D_S} = C_{D_{S-PR}} + C_{D_{S-sec}} \quad , \tag{58a}$$

$$C_{D_{S-PR}} = 0.016 \quad , \tag{58b}$$

$$C_{D_{S-sec}} = 0.018 \, C_{L_S}^{*2} \quad . \tag{58c}$$

The optimum lift coefficient used in equation (58c) is obtained from:[4]

$$C_{L_S}^* = 2 \left[ \frac{1 + \left( \dfrac{\pi(1 - X_H) - 4\,\varepsilon_s\emptyset}{4\emptyset} \right)^2}{1 + \left( \dfrac{\pi(1 - X_H^2)}{4\emptyset} \right)^2} \right]^{1.375} \tag{59}$$

If only prerotators are used then,[4]

$$\varepsilon_p = \varepsilon_{imp} \quad \text{and} \quad \varepsilon_s = 0 \quad , \tag{60}$$

and also,[4]

$$\frac{\Delta\Psi_p}{\Psi_{th}} = \frac{C_{D_p}^* \, \emptyset}{\sin^2 \gamma_p} \cdot \frac{2}{\pi(1 - X_H^2)} \quad (\text{for } 0.7 \le \varepsilon_p < 1.5) \, , \tag{61a}$$

or[4]

$$\frac{\Delta \Psi_p}{\Psi_{th}} = \frac{C_{D_p}* \, \emptyset}{3 \, \epsilon_p \, \sin^3 \gamma_p} \cdot \frac{4}{\pi(1 - X_H^2)} \quad (\text{for } \epsilon_p < 0.7),$$ (61b)

where

$$\gamma_p = \cot^{-1}\left(\frac{\epsilon_p}{2}\right) \quad .$$ (62)

The prerotator drag coefficient $C_{D_p}$ is calculated exactly as in equation (58). The optimum lift coefficient of equation (58c) now becomes,[4]

$$C_{L_p}* = 2\left[\frac{1 + \left(\frac{\pi(1 - X_H^2)}{4\emptyset}\right)^2}{1 + \left(\frac{\pi(1 - X_H^2) + 4 \, \epsilon_p \emptyset}{4\emptyset}\right)^2}\right]^{1.375} \quad .$$ (63)

The clearance losses can be avoided with proper sealing of the straightener or prerotator blades to the casing. Thus, the annulus drag component need not be considered since it will be small.

The pressure loss associated with the diffusion process can be obtained by assuming the diffusion efficiency. Provided flow separation is avoided, diffuser efficiencies of $\eta_D = 0.8$ are obtainable and will be assumed in the calculations. For an annular-type diffuser, as shown in figure 10, in which $\theta_D \cong 3°$, the diffusion pressure loss coefficient ($\Delta \Psi_D$) is,[4]

$$\Delta \Psi_D = (1 - \eta_D)\left[1 - \left(\frac{A_{imp}}{A_{duct}}\right)^2\right] \cdot \frac{\eta_T \, V_{ax}^2}{2 \, V_{tip}^2} \quad ,$$ (64)

where

$A_{imp}$ = Impeller annulus area

$A_{duct}$ = Diffuser outlet or duct area.
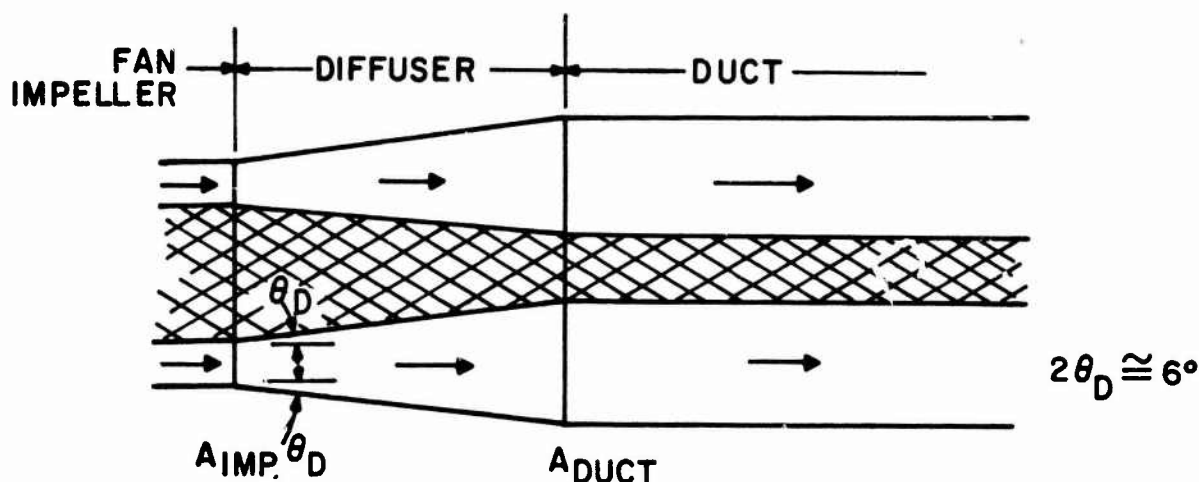
Figure 10
Annular Diffuser

If the duct diameter of the fan unit remains constant, the loss coefficient becomes,[4]

$$\Delta\Psi_D = (1 - \eta_D)\left[X_H^2\,(2 - X_H^2)\right] \cdot \frac{\eta_T\,V_{ax}^2}{2\,V_{tip}^2}\ . \tag{65}$$

The efficiency loss associated with the diffusion is obtained by dividing equation (64) or (65) by (43).

The fan total efficiency may now be determined from:

$$\eta_T = \eta_{imp} - \frac{\Delta\Psi_D}{\Psi_{th}} - \frac{\Delta\Psi_s}{\Psi_{th}}\left(\text{or } \frac{\Delta\Psi_p}{\Psi_{th}}\right)\ . \tag{66}$$

If the $\eta_T$ calculated in equation (66) differs by more than ~5% from the value of $\eta_T$, assumed initially in equation (44), repeat the calculation substituting the new value of $\eta_T$ in equation (44) and repeating all calculations up to this point. If the $\eta_T$ calculated is within 5% of the $\eta_T$ assumed, then the initial design assumptions are reasonable and design calculations may continue.

27-404                              38

# DETAILED DESIGN

At this point, the preliminary fan design is completed and the detailed fan design will be undertaken. Two design methods are available, the isolated airfoil method or the cascade design method. For solidity values below 0.7, the isolated airfoil data are used, while for solidity above 1.0 the cascade data are used. In between, either method may be used. Wallis[4] also recommends that the straighteners or prerotators be designed by the cascade method only. For the design of all blade elements, free vortex flow is assumed, that is, constant axial velocity along the blades.

In designing the impeller blading, an airfoil section must be chosen such as one of the NACA profiles. In the detailed design, only the lift coefficient ($C_L$) and the angle of attack ($\alpha$) for the design point are required. When the detailed design is completed, the complete airfoil section characteristic data will be needed to calculate off-design performance.

## PREROTATOR DESIGN

If prerotators are used, their design must be determined before the impeller design can be finalized. To define the blade shape, it is divided into an even number of segments of equal length. An even number of segments will also provide specifications of the blade at a midspan location which is required for the off-design characteristics. Thus,

$$D_i = D_H + \frac{(D_{tip} - D_H)}{j} \sum_{i=0}^{j} i \quad , \qquad (67)$$

where j is an even number of blade sections and i denotes the diameter location from the hub to the tip of the blade. The ratio of section-to-tip diameter is expressed by:

$$X_i = \frac{D_i}{D_{tip}} \quad (\text{for } i = 0 \text{ to } j) \quad . \qquad (68)$$

27-404                    39

Likewise, the flow coefficient at each section diameter is expressed by:

$$\phi_i = \frac{\phi_{tip}}{x_i} \quad (\text{for } i = 0 \text{ to } j) . \tag{69}$$

The prerotator swirl coefficient is then

$$\epsilon_{p_i} = \frac{\epsilon_{imp_{tip}}}{x_i} \quad (\text{for } i = 0 \text{ to } j) , \tag{70}$$

and the relative velocity of the flow coming off the prerotator is at an angle $(\delta_p)$ with respect to the axis of rotation, defined by:

$$\delta_{p_i} = \tan^{-1} (\epsilon_{p_i}) \quad (\text{for } i = 0 \text{ to } j) . \tag{71}$$

The solidity at each section for the prerotator is determined by:[4]

$$\sigma_{p_i} = \frac{2}{3} \quad (\text{for } \epsilon_{p_i} < 0.7) , \tag{72a}$$

and

$$\sigma_{p_i} = \frac{2 \epsilon_{p_i} \sin \gamma_{p_i}}{C_L} \quad (\text{for } 0.7 \leq \epsilon_{p_i} < 1.5) , \tag{72b}$$

and Wallis[4] assumes that with prerotators, $C_L = 2$ satisfies most cases.

The camber angle (see figure 8) of the prerotator blade at each section is obtained from:[4]

$$\theta_{p_i} = \frac{\delta_{p_i}}{1 - 0.2/\sigma_{p_i}} \quad (\text{for } i = 0 \text{ to } j) . \tag{73}$$

The blade chord is equal to,

$$c_{p_i} = \frac{\pi D_i \, \sigma_{p_i}}{N_p} \,, \tag{74}$$

where $N_p$ is the number of prerotator blades. In general, it is recommended that the number of prerotator or straightener blades be greater than the number of impeller blades.[5,15] Stricker and Shank[15] recommend that the number of straightener or prerotator blades be two more than the number of impeller blades for optimized noise considerations.

$$N_p = N_s = N_{imp} + 2 \,. \tag{75}$$

In order to facilitate manufacturing of the prerotator blades, the blade chord and/or the blade camber angle may be kept constant. The values of $C_p$ and $\theta_p$ would be set at the values calculated for the midspan and new $\sigma_{p_i}$, $\delta_{p_i}$, and $\epsilon_{p_i}$ coefficients must be calculated by using equations (74), (73), and (71), respectively.

IMPELLER DESIGN

The impeller design will depend on whether prerotators or straighteners are used. The impeller blade is broken into sections along its diameter equal to those used for the prerotator or straightener section. Thus, equations (67), (68), and (69) apply for calculating $D_i$, $X_i$, and $\emptyset_i$, respectively. If no prerotators are used, then $\epsilon_{p_i}$ equals zero for the design point on the impeller. However, if prerotators only are used, $\epsilon_{s_i}$ equals zero at the design point unless the prerotator blades were modified to have constant $C_p$ and/or $\theta_p$ to facilitate manufacturing. In this case, there may be a swirl component coming off the blade at the design point and thus $\epsilon_{s_i} \neq 0$. The swirl coefficient calculated for the modified prerotator must be subtracted from,

$$(\epsilon_s + \epsilon_p)_i = \frac{\epsilon_{imp_{tip}}}{X_i} \,, \tag{76}$$

in order to determine $\epsilon_{s_i}$. If the prerotator blade has not been modified, $\epsilon_{s_i}$ equals zero at the design point.

The product of lift coefficient ($C_L$) and solidity ($\sigma_{imp_i}$) can be expressed by,[4]

$$C_L \, \sigma_{imp_i} = 2 \, (\epsilon_s + \epsilon_p)_i \, \sin \gamma_{imp_i} \, . \tag{77}$$

where $\gamma_{imp}$ is shown in figure 9 and determined by,[4]

$$\gamma_{imp_i} = \tan^{-1} \left[ \frac{4\phi_i}{\pi(1 - X_H^2) - 2 \, (\epsilon_s - \epsilon_p)_i \, \phi_i} \right] . \tag{78}$$

At this point, the lift coefficient ($C_L$) is selected from the characteristic of the airfoil to be used. The angle of attack ($\alpha$) at which it occurs is also noted. Then, dividing equation (77) by the value of $C_L$ selected, the solidity ($\sigma_{imp_i}$) is determined. The blade chord is then obtained by,

$$c_{imp_i} = \frac{\pi D_i \, \sigma_{imp_i}}{N_{imp}} \, . \tag{79}$$

If the number of impeller blades ($N_{imp}$) is not specific, it may be approximated from the hub-to-tip ratio ($X_H$) given by,[16]

$$N_{imp} = \frac{6X_H}{(1 - X_H)} \, . \tag{80}$$

The blade angle ($\beta_i$) is determined by,

$$\beta_i = (\gamma_{imp_i} + \alpha) \tag{81}$$

## STRAIGHTENER DESIGN

If the design includes the straighteners only, then $\epsilon_p = 0$ and thus,

$$\epsilon_{s_i} = \frac{\epsilon_{imp_{tip}}}{X_i} \quad . \tag{82}$$

The solidity is obtained from:[4]

$$\sigma_{s_i} = \frac{2}{3} \quad (\text{for } \epsilon_{s_i} \leq 0.5) \quad , \tag{83a}$$

or

$$\sigma_{s_i} = \frac{2 \epsilon_{s_i} \sin \gamma_{s_i}}{(2.18 - 1.43 \epsilon_{s_i})} \quad (\text{for } \epsilon_{s_i} > 0.5) \quad . \tag{83b}$$

The camber angle of the blade is determined from:[4]

$$\theta_{s_i} = \frac{\delta_{s_i}}{1 - 0.26\sqrt{\frac{1}{\sigma_{s_i}}}} \quad , \tag{84}$$

where

$$\delta_{s_i} = \tan^{-1} (\epsilon_{s_i}) \quad . \tag{85}$$

The straightener blade chord is

$$c_{s_i} = \frac{\pi D_i \, \sigma_{s_i}}{N_s} \quad , \tag{86}$$

where $N_s$ is the number of straightener blades as defined in equation (75). As before, the values of $c_s$ and/or $\theta_s$ can be kept constant at their midspan value to facilitate manufacturing. However, new $\sigma_{s_i}$, $\delta_{s_i}$, and $\epsilon_{s_i}$ values must be determined from equations (86), (84), and (85), respectively.

## OFF-DESIGN PERFORMANCE PREDICTION

The off-design performance details the pressure-flow characteristics of the fan at a given speed for other than the design flow condition. The basic assumption of the off-design theory is that conditions at the midspan of the blades are representative of the fan as a whole. Depending on the solidity values calculated earlier, it will be known whether isolated or cascade airfoil data should be used. The data required from the selected blade characteristic are the angle of attack ($\alpha$) and the corresponding lift coefficient ($C_L$), and lift-to-drag ratio ($C_L/C_D$). Several angles of attack on both sides of the design point should be selected to describe fully the fan characteristic curve.

The angle between the mean relative velocity to the impeller and the plane of rotation ($\gamma_{imp}$) is defined by:

$$\gamma_{imp} = (\beta_m - \alpha) . \tag{37}$$

The angle is then used to calculate the swirl coefficients,[4]

$$(\epsilon_s + \epsilon_p) = \frac{C_L \, \sigma_{imp}}{2 \sin \gamma_{imp}} \left[ 1 + \frac{\cot \gamma_{imp}}{(C_L/C_D)} \right] . \tag{88}$$

The value of $\epsilon_s$ or $\epsilon_p$ is obtained from the detailed design section for the midspan of the straightener or prerotator, depending on which is used. If straighteners are used, the value of $\epsilon_p$ is assumed to equal zero which means no preswirl is occurring prior to the impeller, which greatly simplifies the math involved without significantly affecting the results.[4] However, if prerotators are used, $\epsilon_s$ can be nonzero due to the swirl component coming off the impeller blades at off-design flows. This can easily be determined since $\epsilon_p$ would already be known. Thus, the flow coefficient can now be calculated at midspan from,[4]

$$\emptyset_m = \frac{\tan \gamma_{imp}}{\left[1 + 0.5*(\epsilon_s - \epsilon_p) \tan \gamma_{imp}\right]} \quad . \tag{89}$$

The theoretical pressure coefficient will be,

$$\Psi_{th} = \frac{2(\epsilon_s + \epsilon_p)}{\emptyset_m} \cdot \frac{V_{ax}^2}{2 V_{tip}^2 \eta_T} \quad . \tag{90}$$

The fan system total efficiency can now be expressed by,[5]

$$\eta_T = 0.98 - \frac{\emptyset_m}{\sin^3 \gamma_{imp}} \left[\frac{1}{\left(\frac{c_L}{c_D}\right) + \cot \gamma_{imp}} + \frac{1}{\frac{55.5}{c_L} + \cot \gamma_{imp}}\right]$$

$$- \frac{\Psi_p}{\Psi_{th}} \left(\text{or } \frac{\Psi_s}{\Psi_{th}}\right) \quad , \tag{91}$$

where

$$\frac{\Psi_p}{\Psi_{th}} = \text{prerotator loss} = \frac{\emptyset_m}{\sin^3 \gamma_p}\left(\frac{\epsilon_p}{\epsilon_p + \epsilon_s}\right) \cdot \frac{c_D}{c_L}$$

$$\tag{92a}$$

or

$$\frac{\Psi_s}{\Psi_{th}} = \text{straightener loss} = \frac{\emptyset_m}{\sin^3 \gamma_s} \cdot \frac{c_D}{c_L} \quad . \tag{92b}$$

27-404          45

The flow through the fan is calculated by,

$$Q = \frac{\pi \, D_{tip}^2}{4} \, (1 - X_H^2) \, V_{tip} \, X_m \, \phi_m \quad . \tag{93}$$

The total pressure of the fan is,

$$P_T = \frac{\rho}{g_c} \, V_{tip}^2 \, \Psi_{th} \quad . \tag{94}$$

The horsepower required to operate the fan is

$$hp = \frac{P_T * Q}{550 * \eta_T} \quad . \tag{95}$$

COMPARISON OF PREDICTED RESULTS

Several sample calculations were performed with the axial fan characteristic program that has just been summarized. The base preliminary design data were:

$$D_{tip} = 4.5 \text{ ft}$$

$$D_{hub} = 2.25 \text{ ft}$$

$$V_{tip} = 400 \text{ ft/sec}$$

$$P_{T_{des}} = 36.0 \text{ lb/ft}^2$$

$$Q_{des} = 1250 \text{ ft}^3/\text{sec.}$$

For the above data, the fan characteristics were predicted for the case with prerotators and with straighteners, as shown in figure 11. The figure shows that with prerotators, a flatter characteristic curve is obtained which is desirable for SEVs. However, its peak efficiency is lower that for the case with straighteners. These data were determined from the characteristics of a RAF 6E blade section such as shown in figure 12.
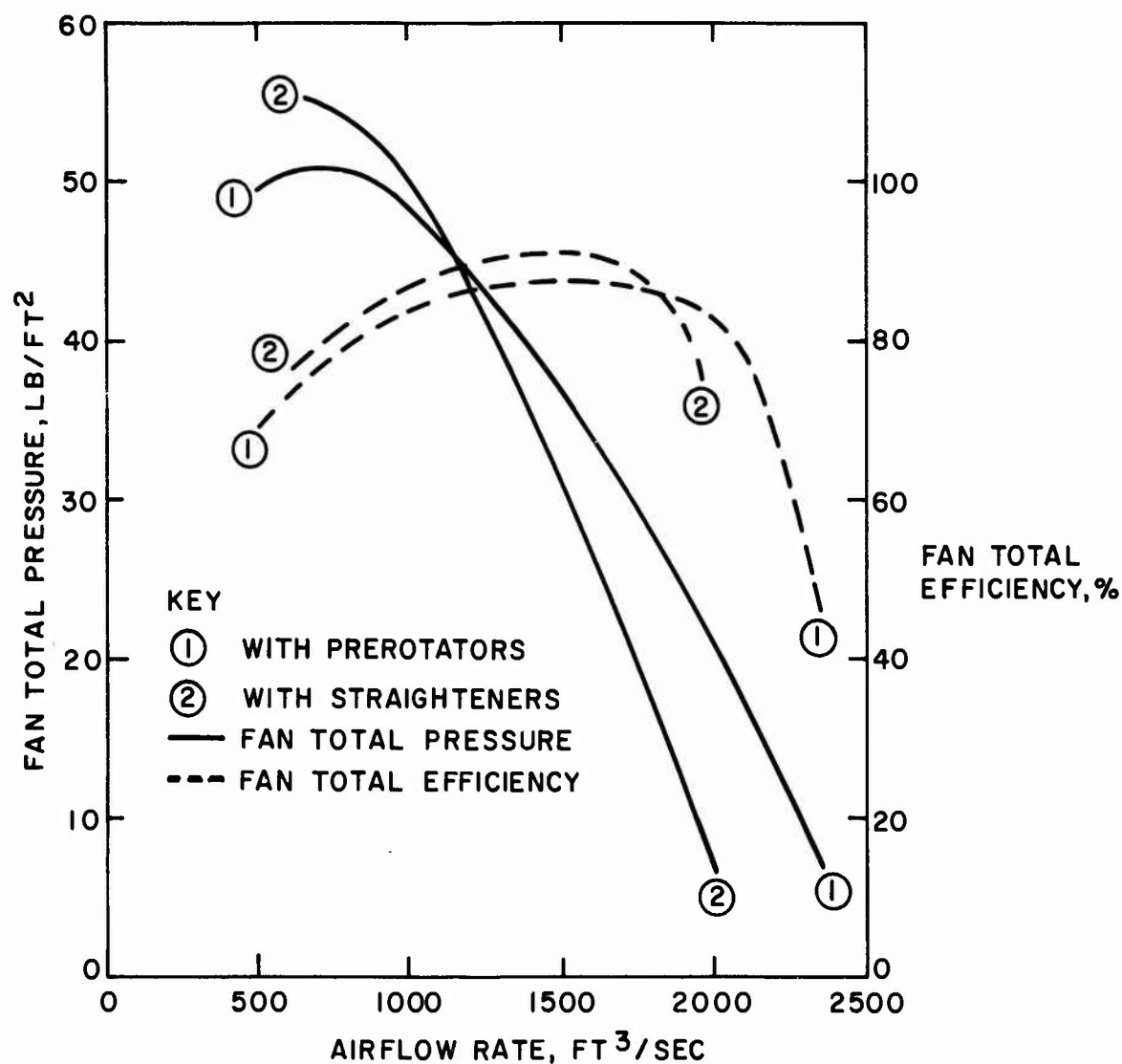


Figure 11
Comparison of Similar Fan Designs with
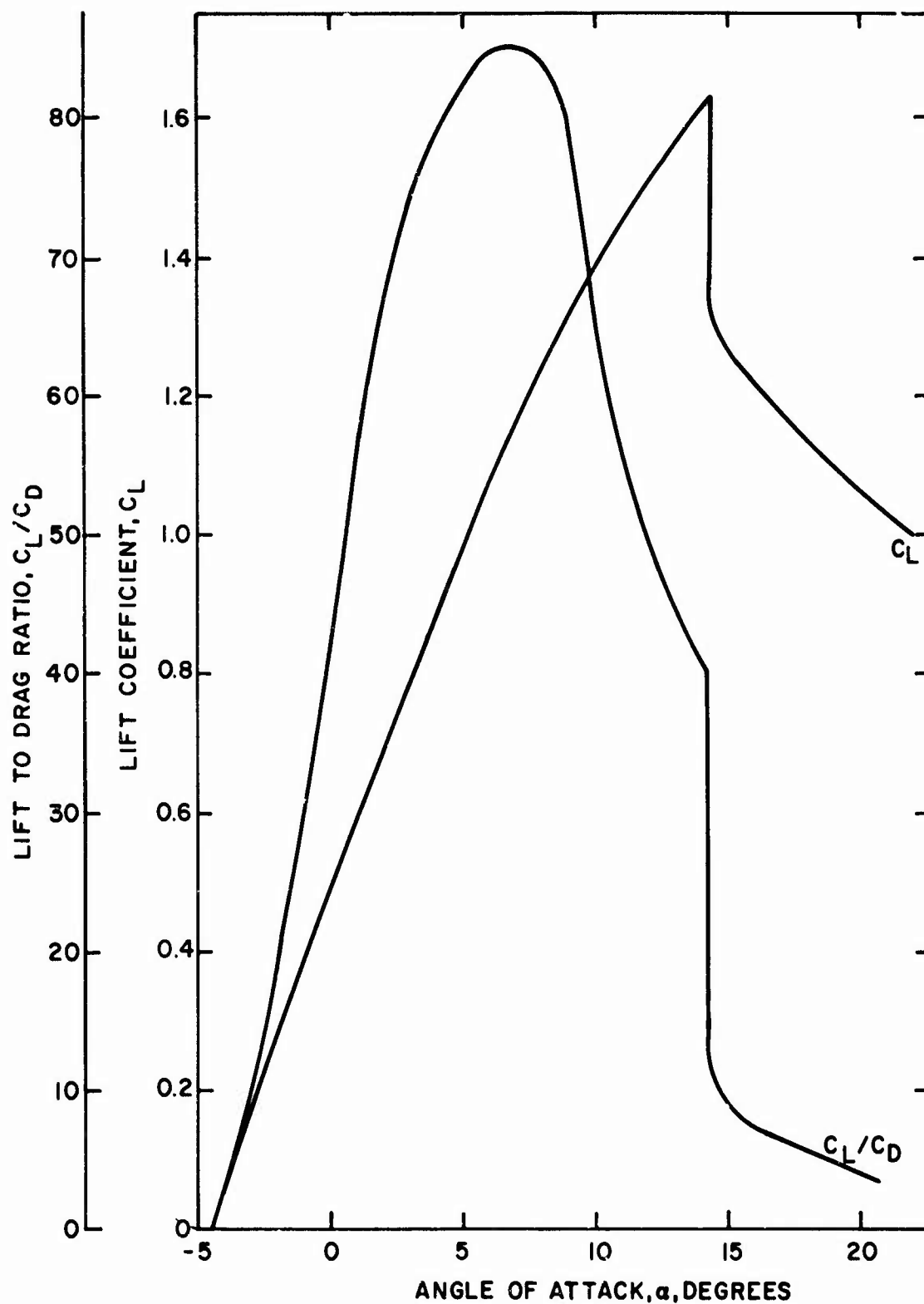Prerotators and with Straighteners

Figure 12
Characteristics of RAF 6E Section

To determine the effect of blade characteristics on the resultant pressure-flow characteristics, a NACA blade profile whose data are shown in figure 13 was used for the same base preliminary design data as the RAF 6E section. Items (a) and (b) of figure 14 show the comparative results for the two blade profiles with prerotators and with straighteners, respectively. The difference between the predicted results for the two blade profiles is significant. The NACA 65 series profile provides the flatter, more desirable pressure-flow characteristic for SEV use. However, its peak efficiency is slightly lower.

In the selection of the most suitable airfoil section for the impeller, three main properties of the section are important to examine.

● $C_L$ - The lift coefficient determines both the solidity of the impeller and the slope of the pressure-flow characteristic. High values of $C_L$ are advantageous in providing both low solidity and low slope.

● $C_L/C_D$ - The lift-to-drag ratio tends to give high efficiencies for high values of the ratio.

● $\alpha_{st} - \alpha_o$ - The difference in angle of attack between stall and zero lift tend to yield increased operating range and reduced characteristic slope at high values of the difference.

The effects of fan diameter on the fan characteristics are shown in items (a) and (b) of figure 15 for an axial fan with prerotators and with straighteners, respectively. Increasing the tip diameter (or decreasing the hub-to-tip ratio) will decrease the slope of the fan characteristic and also lower peak fan total efficiency. The figures also include an estimate of how the basic axial fan weight will vary for the change in variables compared to the base fan design of curve 2. The axial fan weight rational was obtained from reference 1.

LIMITATIONS OF THE AXIAL FAN PREDICTION PROGRAM

In the axial fan prediction program, the number of impeller blades does not affect the fan performance other than to increase or decrease chord length. This is not absolutely true and experience must be relied on not to choose too many or too few blades. This program is intended to be used in the range of incompressible flow for an axial fan having either straighteners or prerotators, but not both.

Figure 13
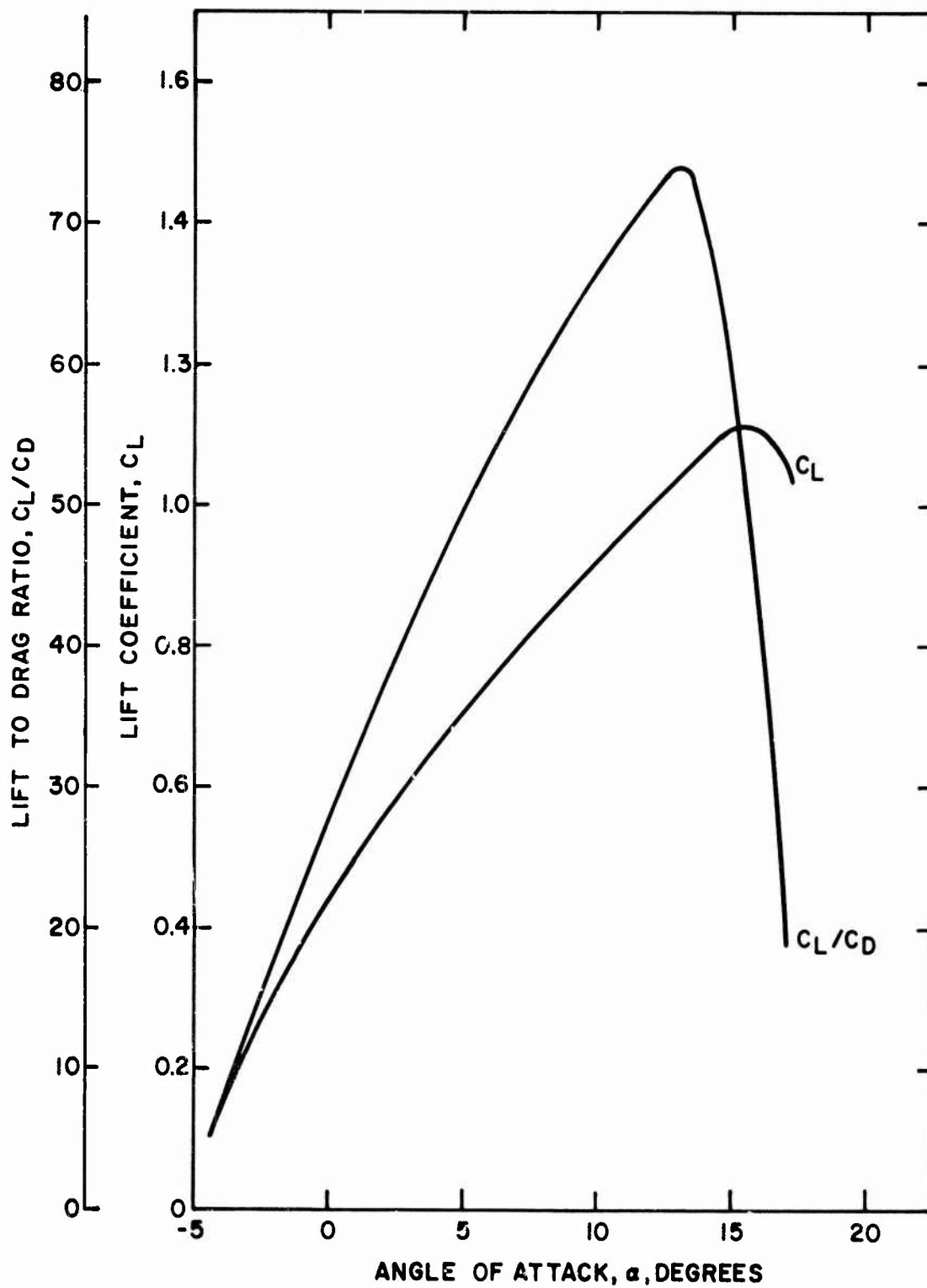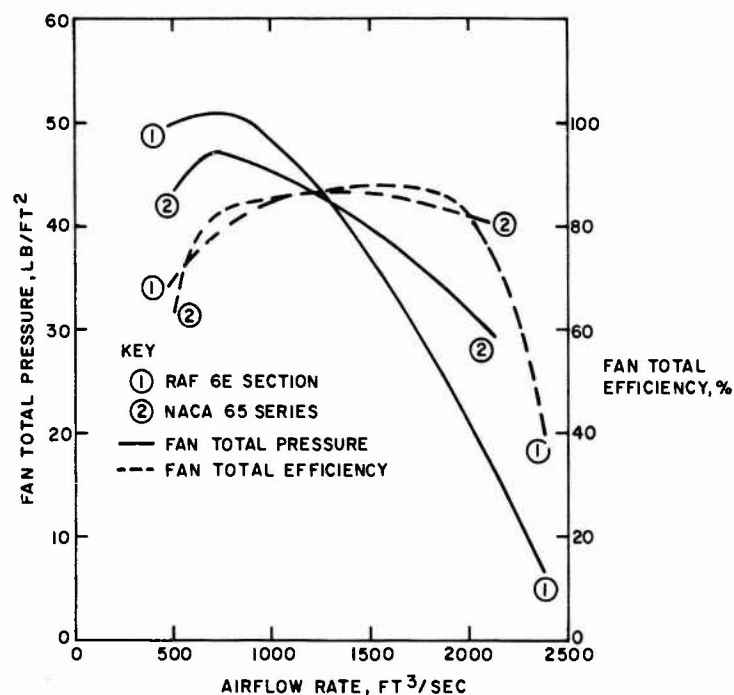Characteristics of NACA 65-(12)10 Section

Item (a)
Comparison of Two Blade Profiles with Prerotators



Item (b)
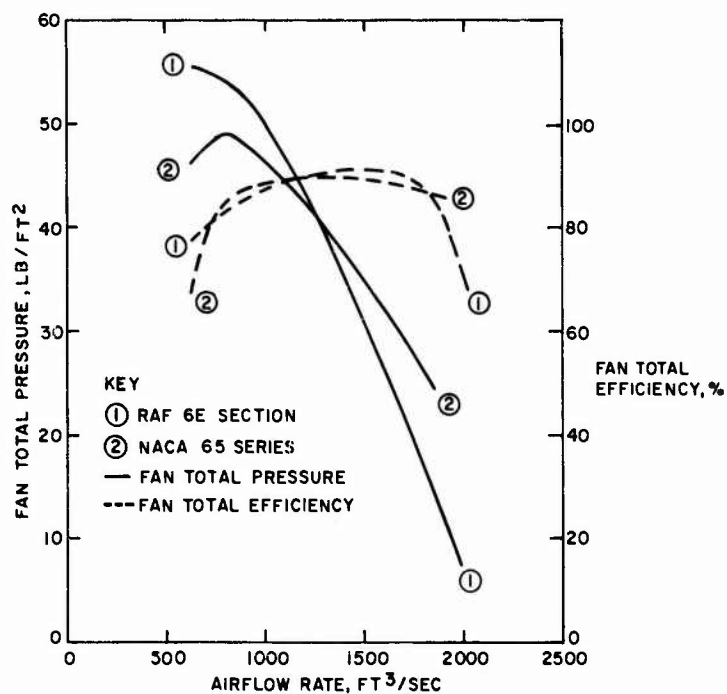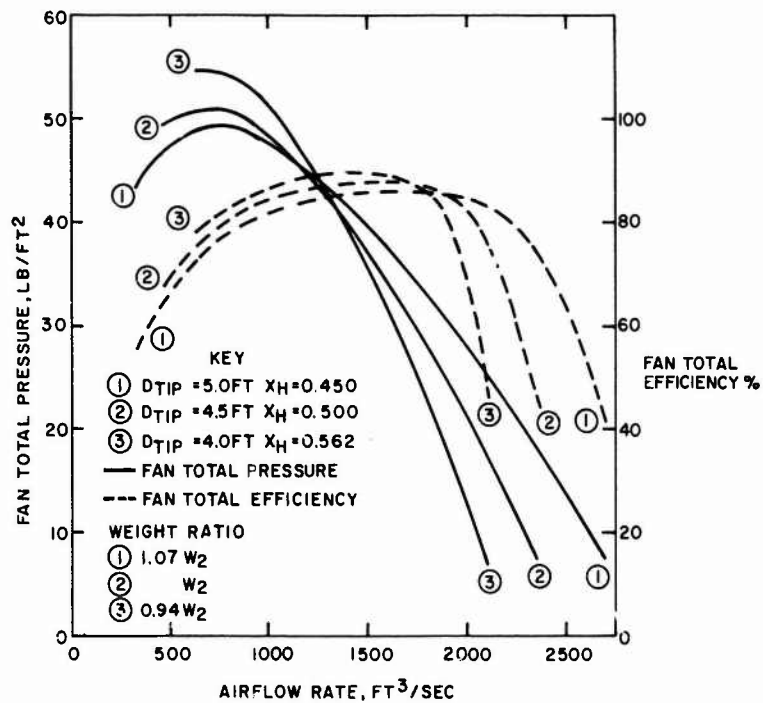Comparison of Two Blade Profiles with Straighteners



Figure 14
Effects of Blade Profile on Axial Fan Performance

Item (a)
Effects of Tip Diameter and Prerotators



Item (b)
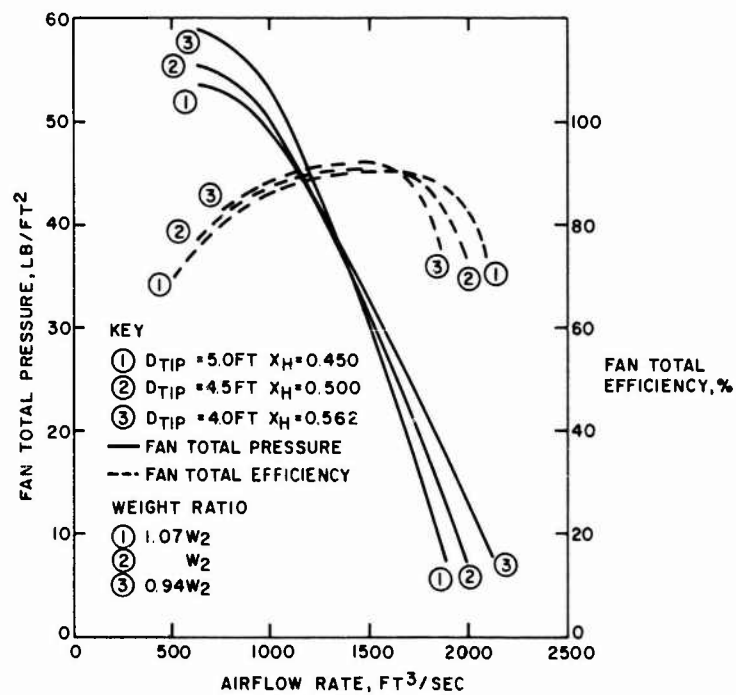Effects of Tip Diameter and Straighteners



Figure 15
Effects of Tip Diameter on Axial Fan Performance

The axial fan prediction program was not compared directly with experimental data due to the lack of suitable data for comparison. Suitable experimental data require knowing what blade profile section was used, a fact which is not included in any obtainable experimental data to date. Shipway[5] claims success in applying a very similar design method to an actual fan design.

## CONCLUSIONS

The fan characteristic programs provide a relatively uncomplicated means of predicting centrifugal and axial fan performance. With these programs, such things as the effects of design changes on the performance and efficiency can be evaluated. On the basis of using these programs, the following general conclusions were drawn:

- Any modification to a fan which results in a flatter fan characteristic slope also tends to cause some reduction in peak fan-system efficiency.

- A significantly flatter fan characteristic slope for a centrifugal fan with backwardly curved blades can be obtained by allowing the fan inside diameter to approach the outside fan diameter, thus resulting in a narrower fan blade.

- An axial fan with straightener vanes is more efficient than a similar fan with prerotator vanes. However, an axial fan with prerotator vanes has a flatter fan characteristic slope than a similar fan with straightener vanes.

- The selection of the axial fan blade profile or blade characteristics can have a significant effect on the resulting fan characteristic slope.

- Decreasing axial fan hub-to-tip ratio or increasing tip diameter will cause a much flatter fan characteristic slope for similar conditions.

## RECOMMENDATIONS

- The prediction programs should be compared against any suitable experimental data that can be obtained in order to evaluate the programs more completely and to understand the selection of suitable design variables for various cases.

● The effects of various parameters and combinations thereof on the fan characteristic slope require more study.

● The effect of the number of fan blades on the performance of the fans should be evaluated separately in the programs. This may perhaps be done best by expressing it as a frictional type of loss.

## TECHNICAL REFERENCES

1 - Purnell, J. G., "Evaluation of Potential Fan Concepts and the Lift Fan Requirements for Large SEV's," NSRDC/A Rept 27-182 (Aug 1972)

2 - Osborne, W. C., Fans, London, England, Pergamon Press (1966)

3 - Shipway, J. C., "Estimation of Head-Flow Curves for Centrifugal Fans," National Physical Lab rept (Oct 1968)

4 - Wallis, R. A., Axial Flow Fans, London, England, Academic Press (1961)

5 - Shipway, J. C., "Aerodynamic Design of Axial Lift Fans," National Physical Lab rept (July 1968)

6 - Shepherd, D. G., Principles of Turbomachinery, New York, The MacMillan Co. (1956)

7 - Wislicenus, G. F., Fluid Mechanics of Turbomachinery, New York, McGraw-Hill Book Co. (1947)

8 - Galvas, M. R., "Analytical Correlation of Centrifugal Compressor Design Geometry for Maximum Efficiency with Specific Speed," NASA TN-D-6729 (Mar 1972)

9 - Csaky, T. G., "A Synthesis of Fan Design for Air Cushion Vehicles," NSRDC Rept 3599 (Oct 1972)

10 - Stodola, A., Steam and Gas Turbines, New York, McGraw-Hill Book Co. (1927)

11 - Brotherhood, P., "Development of Improved Fans for the Britten Norman CC2-001 Cushion Craft," Royal Aircraft Establishment Tech Rept 66271 (Aug 1966)

12 - Shank, S. R., and J. S. Houston, "10-Ton SEV Obstacle Crossing Data Related to Cushion System Dynamics," NSRDC/A Rept 27-229 (Aug 1972)

13 - Csanady, G. T., Theory of Turbomachines, New York, McGraw-Hill Book Co. (1964)

14 - Emery, J. C., et al, "Systematic Two-Dimensional Cascade Tests of NACA 65-Series Compressor Blades at Low Speeds," NASA Rept TR-1368 (1958)

15 - Stricker, J. G., and S. R. Shank, "Development of Noise-- Optimized, Mixed-Flow Pumps for Main Sea-Water and Proposed Hovering Systems," NSRDC/A Rept C183 (Aug 1969)

16 - Fan Engineering, 5th edition, Buffalo, New York, Buffalo Forge Co. (1966)

APPENDIX A

CENTRIFUGAL FAN CHARACTERISTIC
PREDICTION PROGRAM

27-404

```
PROGRAM  TCOGE                CDC 6600 FTN V3.0-P308 CPT=0   06/20/73   15.32.58.        PAGE   1

C        PROGRAM CENTFAN(INPUT,OUTPUT,TAPE1=INPUT,TAPE3=OUTPUT)
C
C        ESTIMATION OF PRESSURE-FLOW CURVES FOR CENTRIFUGAL FANS
C
C        U2 = FAN SPEED - RPM
C        D1 = INSIDE DIAMETER - FT.     (INPUT IN INCHES)
C        D2 = OUTSIDE DIAMETER - FT.    (INPUT IN INCHES)
C        B1 = INSIDE BLADE HEIGHT - FT. (INPUT IN INCHES)
C        B2 = OUTSIDE BLADE HEIGHT - FT. (INPUT IN INCHES)
C        A1 = INLET BLADE ANGLE - DEGREES
C        A2 = OUTLET BLADE ANGLE - DEGREES
C        Z  = NUMBER OF BLADES
C        E  = VOLUTE OUTLET AREA - FT**2   (INPUT IN SQUARE INCHES)
C
10       READ(1,15)
15       D2,D1,B2,B1,D2,Z,A1,A2,E
         D1 = D1/12.
         D2 = D2/12.
         B1 = B1/12.
         B2 = B2/12.
         U2 = U2*3.1416*(D2/60.)
         VKTF(3,915) U2,D1,B1,A1,B2,B2,A2,Z,E
         U = 3.1416
         D1 = D*D1*B1
         D2 = U*D2*B2
         A1 = A1*.01745
         A2 = A2*.01745
         CD = D1/D2
         DE = D1/D2
C
C        FLOW RANGE AND INCREMENTS
C
         QGMAX = ABS(U2*C2*TAN(A2))
         IQSTEP = QGMAX/25.
         DO 180 IQ = 1,IQMAX,IQSTEP
         Q = IQ - 1
180      F = Q/(C2*C2*U2)
C
C        EULER LINE - IDEAL PRESSURE
C
         VU2 = 12. - Q/(C2*TAN(A2))
         FL2 = U2*U2*VU2
         F1 = 1. - F*C2/(B*F2*TAN(A2))
C
C        BLADING LOSSES
C
         CVU2 = F*SIN(A2)*U2/Z
         FLA = U2*B*VU2
         VCA = B/7*FTN(A2)
C
C        DOWNSTREAM DISCHARGE VELOCITY LOSS (SINUSOIDAL)
C
         GF2 = (F*D/B-1.)*B*U2*C/ABS(C2*TAN(A2))
```

27-404                                    A-1

```
PROGRAM     CENTRFGA   TESDE

            S22 = (F**F/3.-1.)*F*F2/(3EC(E*P2*TAN(A2))
            F2 = F2A + D2E
            S2 = S2A + S2E

C           IMPELLER LOSS
C
            F2 = C.725*2*RC*(1./(C1*SIN(A1))-1./(C2*SIN(F2)))**2
            C3 = C.17F*(F*C2/(F*A2))**2*(1./(G*RB*SIN(A1))-1./SIN(A2))**2

C           INLET LOSSES (EXPANSION + TURNING)
C
            AK = C.78
            B4 = AK*F/2. * (4./FBC/(1.9*C1)**2)**2
            C4 = AK/2.*F*F*(4./(.8*C1/(.C2/(.8*C1)**2)**2

C           PLADE INLET LOSSES (EXPANSION OF CONTRACTION LOSS + TURNING LOSS
C           CLF TO P2F-SWIRL)
C
            AK = 0.7
            X = 4.*R/(C*B1*C1)
            Y1 = ((C/C1)**2 + (L2*RC-C/C1)**2)**.5
        710 TF(X-Y1) 310,310,340
            S = TAN(40.*C.01745)
            GC TO 760
        740 FE = PK*F/2.*(4.*C/(C*C1*C1)-((C/C1)**2+(U2*RO-C*S/C1)**2)**.5)**2
        760 SE = CK/2.*(4.*C*S/RFW/2-((C2*F/(RO*RO*F*R2)**2*(1.+S*S)-2.*C2*F*S
            1/(C*RF*R2)+C*C2)*C*(*)**.5)**2
            VL2P = VL2 - CVL2
            V2P = (VL2P**2 + (C/C2)**2)**.5

C           FAN PRESSURE
C
            T = F1 - P2 - F3 - F4 - F5
            TF(T) 620,620,400
        400 T1 = S1 - S2 - S3 - S4 - S5

C           LEAKAGE LOSS
C
        410 IF(E)415,480,410
            C1 = .6*F*C1*C1*0.005*(2.*T/P)**.5
            F1 = .0025*RC*RF*R*(2.*T1)**.5
            C2 = C-C1
            F2 = F-F1
        420 IF(C) 435,427,425
            C = C1
            GC TO 185

C           OUTLET LOSSES (EXPANSION LOSS)
C
        435 IF(S) 450,450,465
        450 BF = C.
            S4 = 0.
            GO TO 475
        465 F4 = .2*F*(V2P - C2/F)**2
```

```
PROGRAM   CENTFAN   TRACE

C
C
          S4 = .2*(V2P/L2-G3/(F*U2))**2
C
C         LEAKAGE PRESSURE DROP LOSS
C
475   T  = T1 - P6
      G6 = C.3
      P7 = .36*T*CK
      G7 = .36*T1*CV
      T  = T  - P7
      T1 = T1 - G6 - G7
C
C         VELOCITY PRESSURE AT FAN OUTLET
C
480   IF(T) 490,490,485
      PR = .5*C*((C/C2)**2 + VL2F**2)
      SP = ((C/(C2*L2))**2+(VL2P/L2)**2)
      T  = T  - PR
      T1 = T1 - SR
482   IF(T) 600,600,410
      PS = T
      SS = T1
      T  = T  + PR
      T1 = T1 + CR
      GO TO 490
485   PR = .5*C*((C-C1)/6)**2
      SS = ((C-C1)/(3*L2))**2*.6
      PS = T1 - PR
      SS = T1 - SP
490   EFFICIENCY (TOTAL & STATIC)
C
C
495   IF(G-C1)402,402,405
492   C2 = C
      G3 = 0.
      PS = C.
      GO TO 490
495   C2 = (C-G1)/C
500   EF1 = T/(P1-P2)*C2
      EF2 = PS/(P1-P2)*C2
      EF1 = T1/(S1-S2)*C2
      ES2 = SS/(S1-S2)*C2
C
      WRITE(3,600)
      WRITE(3,970) E1, P2A, P2E, F3, F4, F5, F6, P7
      WRITE(3,970) S1, SPA, S2E, S3, S4, S5, S6, S7
      WRITE(3,950)
      WRITE(3,970) C, G3, T, PF1, PA, FS, FP2
      WRITE(3,970) F, F2, T1, FS1, SR, SS, ESP
610   CONTINUE
620   WRITE(3,690) IGMAX
      GO TO 11
C
900   FORMAT(5E8.2)
910   FORMAT(1H1//7X,41HOUTER SPEED =,F0.2,9H FEET/SEC//5X,29HINSIDE   : 0
     1LINETER =,F0.2,94H FEET    BLADE HEIGHT =,F0.2,23H FEET    BLADE
```

A-4

```
PROGRAM   CENTFAN   TRAGE                    CDC 6600 FTN V3.0-P369 OPT=0   06/20/73   15.32.58.

        2 ANGLE =,F9.2,9H DEGREES//5X,7HOUTSIDE,13X,F9.2,24X,F9.2,23X,F9.2,23X,F9.2/
        3/25X,19HNUMBER OF BLADES =,F10.0//25X,13HOUTLET AREA =,F10.2,6H FT
        4**2/)
170 900 FORMAT(//15X,3HE1,15X,3HP2A,12X,3HP2B,12X,2HP3,12X,2HP4,13X,2HF5,
        113X,2HP6,13X,2HP7/)
    960 FORMAT(/11X,2H C,16X,4HG-G1,0X,7HF-TOTAL,8X,0HTOTAL EFF,7X,8HVEL C
        1 1DES,8X,0HSTAT EFF,7X,8HSTAT EFF/)
    970 FORMAT(6X,9F16.6)
175 980 FORMAT(///10X,17H0-MAX %CFAL =,I10)
   1000 STOP
        END
```

TIP SPEED = 233.00 FEET/SEC

INSIDE : DIAMETER = 3.46 FEET    BLADE HEIGHT = 1.62 FEET    BLADE ANGLE = 25.00 DEGREES
OUTSIDE            5.00                         1.18                        50.00

NUMBER OF BLADES = 12.
OUTLET AREA = 21.00 FT**2

| P1 | P2A | P2B | P3 | P4 | P5 | P6 | P7 |
|---|---|---|---|---|---|---|---|
| 125.72328 | 25.35597 | 0.16972 | 0.00063 | 0.00491 | 19.92644 | 15.93469 | 6.94773 |
| 1.98851 | 0.40105 | 0.00268 | 0.00001 | 0.00008 | 0.31517 | 0.25203 | 0.10989 |

| Q | Q-Q1 | P-TOTAL | TOTAL EFF | VEL PRES | STAT PRES | STAT EFF |
|---|---|---|---|---|---|---|
| 29.52888 | 0.0 | 57.38318 | 0.0 | 0.00000 | 57.38318 | 0.0 |
| 0.00684 | 0.0 | 0.90760 | 0.0 | 0.00000 | 0.90760 | 0.0 |

| P1 | P2A | P2B | P3 | P4 | P5 | P6 | P7 |
|---|---|---|---|---|---|---|---|
| 121.47778 | 25.35597 | 1.17828 | 0.03031 | 0.23671 | 13.38191 | 13.30314 | 7.33551 |
| 1.92026 | 0.40105 | 0.01864 | 0.00048 | 0.00374 | 0.21166 | 0.21041 | 0.11602 |

| Q | Q-Q1 | P-TOTAL | TOTAL EFF | VEL PRES | STAT PRES | STAT EFF |
|---|---|---|---|---|---|---|
| 205.00000 | 175.23122 | 60.58592 | 0.54586 | 0.08109 | 60.50482 | 0.54513 |
| 0.04750 | 0.04060 | 0.95826 | 0.54586 | 0.00128 | 0.95698 | 0.54513 |

| P1 | P2A | P2B | P3 | P4 | P5 | P6 | P7 |
|---|---|---|---|---|---|---|---|
| 116.36606 | 25.35597 | 2.36656 | 0.12123 | 0.94685 | 7.53466 | 10.67668 | 7.49780 |
| 1.84051 | 0.40105 | 0.03727 | 0.00192 | 0.01498 | 0.11917 | 0.168C8 | 0.11859 |

| Q | Q-Q1 | P-TOTAL | TOTAL EFF | VEL PRES | STAT PRES | STAT EFF |
|---|---|---|---|---|---|---|
| 410.00000 | 380.44702 | 61.92630 | 0.64817 | 0.38223 | 61.54407 | 0.64417 |
| 0.09500 | 0.08815 | 0.97946 | 0.64817 | 0.00605 | 0.97341 | 0.64417 |

| P1 | P2A | P2B | P3 | P4 | P5 | P6 | P7 |
|---|---|---|---|---|---|---|---|
| 111.32434 | 25.35597 | 3.53483 | 0.27276 | 2.13041 | 3.49242 | 8.35720 | 7.36351 |
| 1.76077 | 0.40105 | 0.05591 | 0.00431 | 0.03370 | 0.05524 | 0.13218 | 0.11647 |

| Q | Q-Q1 | P-TOTAL | TOTAL EFF | VEL PRES | STAT PRES | STAT EFF |
|---|---|---|---|---|---|---|
| 615.00000 | 586.10278 | 60.81720 | 0.70311 | 0.90716 | 59.91003 | 0.69262 |
| 0.14250 | 0.13581 | 0.96192 | 0.70311 | 0.01435 | 0.94757 | 0.69262 |

| P1 | P2A | P2B | P3 | P4 | P5 | P6 | P7 |
|---|---|---|---|---|---|---|---|
| 106.28262 | 25.35597 | 4.71311 | 0.48490 | 3.78741 | 1.07686 | 6.46737 | 6.95487 |
| 1.68103 | 0.40105 | 0.07455 | 0.00767 | 0.05990 | 0.01703 | 0.10229 | 0.11000 |

27-404

A-5

| | Value 1 | Value 2 |
|---|---|---|
| Q | 820.00000 | 0.19000 |
| Q-Q1 | 792.19434 | 0.18356 |
| P-TOTAL | 57.44209 | 0.90854 |
| TOTAL EFF | 0.72814 | 0.72814 |
| VEL PRES | 1.65729 | 0.02621 |
| STAT PRES | 55.78479 | 5.88232 |
| STAT EFF | 0.70713 | 0.70713 |
| P1 | 101.24089 | 1.60128 |
| P2A | 25.35597 | 0.40105 |
| P2B | 5.89139 | 0.09318 |
| P3 | 0.75766 | 0.01198 |
| P4 | 5.91782 | 0.09360 |
| P5 | 0.06761 | 0.00107 |
| P6 | 4.92498 | 0.07790 |
| P7 | 6.29914 | 0.09963 |

| | Value 1 | Value 2 |
|---|---|---|
| Q | 1025.00000 | 0.23750 |
| Q-Q1 | 998.73047 | 0.23142 |
| P-TOTAL | 52.02629 | 0.82288 |
| TOTAL EFF | 0.72425 | 0.72425 |
| VEL PRES | 2.63411 | 0.04166 |
| STAT PRES | 49.39218 | 0.78121 |
| STAT EFF | 0.68758 | 0.68758 |
| P1 | 96.19917 | 1.52154 |
| P2A | 25.35597 | 0.40105 |
| P2B | 7.06967 | 0.11182 |
| P3 | 1.09103 | 0.01726 |
| P4 | 8.52166 | 0.13478 |
| P5 | 1.63417 | 0.02585 |
| P6 | 3.69211 | 0.05840 |
| P7 | 5.27413 | 0.08342 |

| | Value 1 | Value 2 |
|---|---|---|
| Q | 1230.00000 | 0.28501 |
| Q-Q1 | 1206.06079 | 0.27946 |
| P-TOTAL | 43.56039 | 0.68898 |
| TOTAL EFF | 0.66975 | 0.66975 |
| VEL PRES | 3.84127 | 0.06076 |
| STAT PRES | 39.71912 | 0.62822 |
| STAT EFF | 0.61069 | 0.61069 |
| P1 | 91.15744 | 1.44180 |
| P2A | 25.35597 | 0.40105 |
| P2B | 8.24795 | 0.13045 |
| P3 | 1.48501 | 0.02349 |
| P4 | 11.59893 | 0.18346 |
| P5 | 0.63537 | 0.01005 |
| P6 | 5.73293 | 0.04323 |
| P7 | 4.43893 | 0.07021 |

| | Value 1 | Value 2 |
|---|---|---|
| Q | 1435.00000 | 0.33251 |
| Q-Q1 | 1413.13110 | 0.32744 |
| P-TOTAL | 36.66232 | 0.57987 |
| TOTAL EFF | 0.62730 | 0.62730 |
| VEL PRES | 5.27353 | 0.08341 |
| STAT PRES | 31.38879 | 0.49646 |
| STAT EFF | 0.53707 | 0.53707 |
| P1 | 86.11572 | 1.36206 |
| P2A | 25.35597 | 0.40105 |
| P2B | 9.42622 | 0.14909 |
| P3 | 1.93960 | 0.03068 |
| P4 | 15.14962 | 0.23962 |
| P5 | 0.11088 | 0.00175 |
| P6 | 2.00235 | 0.03167 |
| P7 | 3.47015 | 0.05489 |

| | Value 1 | Value 2 |
|---|---|---|
| Q | 1640.00000 | 0.38001 |
| Q-Q1 | 1620.70215 | 0.37554 |
| P-TOTAL | 28.66090 | 0.45332 |
| TOTAL EFF | 0.55176 | 0.55176 |
| VEL PRES | 6.93654 | 0.10971 |
| STAT PRES | 21.72437 | 0.34360 |
| STAT EFF | 0.41822 | 0.41822 |
| P1 | 81.07401 | 1.28231 |
| P2A | 25.35597 | 0.40105 |
| P2B | 10.60450 | 0.16773 |
| P3 | 2.45481 | 0.03883 |
| P4 | 19.17374 | 0.30326 |
| P5 | 0.01334 | 0.00021 |
| P6 | 1.45841 | 0.02307 |
| P7 | 2.37743 | 0.03760 |

| | Value 1 | Value 2 |
|---|---|---|
| Q | 1845.00000 | 0.42751 |
| Q-Q1 | 1828.99731 | 0.42380 |
| P-TOTAL | 19.63579 | 0.31057 |
| TOTAL EFF | 0.43148 | 0.43148 |
| VEL PRES | 8.83411 | 0.13973 |
| STAT PRES | 10.80168 | 0.17084 |
| STAT EFF | 0.23736 | 0.23735 |
| P1 | 76.03229 | 1.20257 |
| P2A | 25.35597 | 0.40105 |
| P2B | 11.78278 | 0.18636 |
| P3 | 3.03063 | 0.04793 |
| P4 | 23.67126 | 0.37440 |
| P5 | 0.30227 | 0.00478 |
| P6 | 1.06123 | 0.01679 |
| P7 | 1.16944 | 0.01850 |

APPENDIX B

AXIAL LIFT FAN CHARACTERISTIC
PREDICTION PROGRAM

```
      PROGRAM AXALFAN(INPUT,CLTPLT,TAPE1=INPUT,TAPE3=OUTPUT)

C     AERODYNAMIC DESIGN OF AXIAL LIFT FANS
C
C     PROGRAM WRITTEN FOR JOHN PUFNELL
C     BY
C     JUDY HOUSTCN
C     DECEMBER 1971
C
      DIMENSION HP(8),HT1(8),K1(8),CLAM(8), KTH1(8), NT1(8), SD(7), X(7)
     1     , LAM(7), EP(8), AL2(7),SC(7), THET(7), NC(7), BETA(8),
     2     ES(8), PHIR(8), CLSIG(7), SIG(7), C(7), B(8), DIFF(8),
     3     ARG(8), TA(8), SI(8), ALPHA(8),GAMMA(8), CL1(8),CO(8),
     4     KL(8)
      REAL KRP,KRA,KSPTH,KD,LAM,NC,N,NT,LAMB,KCTH,LAMBAR,NR,KTH,NT1,
     1     KTH1,K1,NT2,ND, NBLAO,KL,KFK,NS
      INTEGER CPT1,CPT2
      PI = 3.1415927
      G = 32.174
      RHO = 0.0767
C
C     READ INPUT
C
  333 READ(1,1020) HT,O,D,CB,VAR,NBLAC,CPT1,CPT2
      IF(HT)334,335,334
  334 WRITE(3,1601) HT,O
 1020 FORMAT(6F10.2,2I1)
 1601 FORMAT(1H1//42X,'HT = ',F10.2,5X,'Q = ',F10.2)
 1602 FORMAT(//42X,'NS = ',F10.3,4X,'OS = ',F10.3)
C     OPT1 = 1 : PRERCTATCR
C     OPT1 = 2 , STRAIGHTENER
C
      XB = OB/D
      IF(NBLAC)341,34C,341
  340 NBLAO = 6.*XB/(1.-XB) + 2.
  341 V = O/(PI*O*C*(1.- XB*XB)/4.)
      NT = -.8
  122 OUT = RHO/G*VTIP*VTIP
      KTH = HT/OUT
C
C     OPT2 = 1 : VAR = N
C     OPT2 = 2 : VAR = VTIP
C
      GO TO (51,52), OPT2
   52 VTIP = VAR
      N = VTIP*60./(PI*O)
      GC TC 60
   51 N = VAR
      VTIP = PI*C*N/60.
   60 BLAM = C/(O*D*VTIP)
      LAMB = BLAM/XB
      EB = 4.*VTIP*VTIP/(FI*V*V*NT*(1.-XB*XB))*KTH*LAMB
      NS = N*PI/30.*C**.5/(G*HT/RHO)**.75
      OS = C*(G*HT/RHO)**.25/0**.5
      WRITE(3,1602)NS,CS
```

```
          GO TO (61,62), OPT1
   61  PHI  = (4.*LAMB  /(PI*(1.-XB*XB)+2.*EB*LAMB  )
       CLSI = 2.*EB*'SIN(PHI )
       CL   = 2.*((1.+ (PI*(1.-XE*XE)/(4.*LAMB   ))**2)/(1.+((PI*(1.-XB*XB)
      1+4.*EB*LAMB  )/(4.*LAMB  ))**2))**1.375
          GO TO 70
   62  PHI  = (4.*LAMB  /(PI*(1.-XE*XB)-2.*EB*LAMB  )
       CLSI = 2.*EB*SIN(PHI )
       CL   = 2.*((1.+((PI*(1.-XB*XB)-4.*EB*LAMB  )/(4.*LAMB   ))**2)/(1.+(
      1PI*(1.-XB*XB)/(4.*LAMB  ))**2))**1.375
   70  SIG1= CLSI /CL
       XBAR = (1.+ XB)/2.
       LAMBAR =  BLAM /XBAR
       EBAR = 4.*VTIP*VTIP/(PI*v*v*NT*(1.-XB*XE))*KTH*LAMBAR
          GO TO (1500,1600), OPT1
 1500  PHIL = (4.*LAMBAR/(PI*(1.-XE*XB)+2.*EB*LAMBAR)
          GO TO 1501
 1600  PHIL = (4.*LAMBAR/(PI*(1.-XE*XB)-2.*EB*LAMBAR)
 1501  GAMKR =LAMBAR/(SIN(PHIL)*SIN(PHIL))*4./(PI*(1.-XB*XB))
       KRP = LAMBAR/(SIN(PHIL)*SIN(PHIL)*20.5)*4./(PI*(1.-XB*XB))
       KRA = .92
       NR = 1. - KRF  - KRA
       CLP = 2.*((1.+ (PI*(1.-XE*XE)/(4.*LAMBAR))**2)/(1.+((PI*(1.-XB*XB)
      1+4.*EB*LAMBAR)/(4.*LAMBAR))**2))**1.375
       COP = 0.016+CLP*CLP*0.018
       CLS = 2.*((1.+((PI*(1.-XE*XE)-4.*EB*LAMBAR)/(4.*LAMBAR))**2)/(1.+(
      1PI*(1.-XB*XB)/(4.*LAMBAR))**2))**1.375
       CDS = 0.016+CLS*CLS*0.018
          GO TO (71,72), OPT1
   71  PHIPS = ATAN(2./EBAR)
       GAMKKT=LAMBAR/(SIN(PHIPS)*SIN(PHIPS))
       IF(EBAR.LT..7) GO TO 81
       KSPTH = CDP*GAMKKT*2./(PI*(1.-XB*XB))
          GO TO 82
   81  KSPTH = CCP*GAMKKT/(3.*EEAR*SIN(PHIPS))*4./(PI*(1.-XB*XB))
          GO TO 82
   72  PHIPS = ATAN(2./EBAR)
       GAMKKT=LAMBAR/(SIN(PHIPS)*SIN(PHIPS))
       IF(EBAR.LT..5) GO TO 91
       KSPTH = CCS*GAMKKT/(2.18-1.43*EBAF)*4./(PI*(1.-XB*XB))
          GO TO 82
   91  KSPTH = CDS*GAMKKT/(3.*EEAR*SIN(PHIPS))*4./(PI*(1.-XB*XB))
   82  NO = .8
       KO = (1. - NO)*(XB*XB*(2. - XB*XB))*NT*v*v/(2.*VTIP*VTIP)
       KOTH = KO/KTH
       NT2 = NR - KOTH   - KSPTH
       NT = NT2
C
C    OUTPUT - TABLE 1
C
  123  WFITE(3,1000)
 1000  FORMAT(  //62X,'TABLE 1'//)
       WPITE(3,1001) C,CB,N,XB,V,OLT,KTH,VTIP,ELAM,LAMB,EB,CLSI ,CL,
      1      SIG1,XBAR,LAMBAR,EBAF,EBAF,GAMKF,KRP,KRA,NR
       KTH = KTH*.8/NT
```

```
1001 FORMAT(/45X,'1  C FAN DIA. (FT)          = ',F5.2/ 45X,'2  DB BOSS DIA (
    1FT)                         = ',F5.0/ 45X,'4  XB
    2                            = ',F5.1/45X,
    3'6 .5*RHO/G*V*V              = ',F5.2/45X,'7  KTH           = ',F5.
    43/45X,'8  VTIP                = ',F5.1/45X,'9  V/VTIP
    5 = ',F5.3/45X, '10 LAMBCAB             = ',F5.3/45X,'11 EB
    6 = ',F5.3/45X,'12 CLSIGMA            = ',F5.3/45X,'13 CL
    7                            = ',F5.3/
    845X, '15 XBAR               = ',F5.3/45X '16 LAMBDA BAR        =
    9',F5.3/45X, '17 ERAR              = ',F5.3/45X, '18 GAMMA*KR/KT
    AH                          = ',F5.2/45X, '19 (KRP + KRS)/KTH  = ',F5.3/45X, '20 KRA
    B/KTH                        = ',F5.3/45X, '21 NR               = ',F5.3/ )
     GO TO(124,125), CPT1
 124 WRITE(3,1002) GAMKKT,KSPTH
1002 FCRMAT(45X,'22 GAMMA*KP/KTH             = ',F5.3/45X,'23 KP/KTH
    1                            = ',F5.3)
     GO TO 126
 125 WRITE(3,1003) GAMKKT,KSFTH
1003 FCRMAT(45X,'22 GAMMA*KS/KTH             = ',F5.3/45X,'23 KS/KTH
    1                            = ',F5.3)
 126 WRITE(3,1004) KO,KOTH,NT2
1004 FORMAT(45X,'24 KC                       = ',F5.3/ 45X,'25 KO/KTH
    1                            = ',F5.3/ 45X,'26 NT               = ',F5.3//)
C
C       TABLE 2A  - PREPCTATOR DESIGN
C
 121 SD(1) = DB
     DO 137 I = 1,5
 137 SD(I+1) = DB + ((D-CB)/6.)*I
     SC(7) = D
     DO 133 I=1,7
     X(I) = SD(I)/C
 133 LAM(I) = BLAM/X(I)
     GO TO(131,132), CPT1
 131 DO 138 I = 1,7
     EP(I) = 4.*VTIP*VTIP/(PI*V*V*NT*(1.-XB*XB))*KTH*LAM(I)
     AL2(I) = ATAN(EP(I)) * 57.2'.7795
     IF(EP(I).LT..7) GO TO 134
     PHI = ATAN(2./EP(I))
     CL = 2.
     SC(I) = CL/(2.*FP(I)*SIN(PHI))
     GO TO 135
 134 SC(I) = 1.5
 135 THET(I) = AL2 (I)/(1. - .2*SC(I))
 138 NC(I) = PI*SD(I)/SC(I)
C
C       CUTPUT - TABLE 2A
C
     WRITE(3,1006)
1006 FCRMAT(/62X,'TABLE 2A'//48X,'1',9X,'2',9X,'3',9X,'4',9X,'5',9X,
    1 '6',9X,'7',/)
     WRITE(3,1007) (SC(I),I=1,7), (X(I),I = 1,7), (LAM(I), I = 1,7),
    1               (THET(I),I =1,7), (NC(I), I = 1,7)
1007 FCRMAT(19X,'1  C (STATIC DIA - FT)',5X,7(F5.2,5X)/ 19X,'2  X',24X,
    1 7(F5.2,5X)/ 19X,'3 LAMBCA',19X, 7(F5.3,5X)/ 19X,'4 EP',23X,
```

```
       2      7(F5.3,5X)/ 19X,'5 ALPHA2',19X, 7(F5.2,5X)/ 19X,'6 S/C',22X,
       3      7(F5.2,5X)/ 19X,'7 THETA', 20X, 7(F5.2,5X)/ 19X,'8 N.C.', 21X,
       4      7(F5.2,5X)//)
170    WRITE(3,1008) NBLAD
1008   FORMAT(19X,'NUMBER OF BLADES - STATCR = ',F5.0//)
       DO 222 I = 1,7
222    ES(I) = EP(I) - 4.*VTIP*VTIF/(PI*V*V*NT*(1.-XB*XB))*KTH*LAM(I)
       GO TO 141
C
175 C   TABLE 2B
C
132    DO 148 K = 1,7
       ES(K) = 4.*VTIP*VTIP/(PI*V*V*NT*(1.-XB*XB))*KTH*LAM(K)
148    EP(K) = 0.
141    READ(1,1009) CL,(ALPHA(I),I=1,7)
180 1009 FORMAT(8F10.3)
       DO 145 K = 1,7
       OIFF(K) = ES(K) - EP(K)
       APG(K) = (PI*(1.-XB*XB)-2.*CIFF(K)*LAM(K))/4.
       TA(K) = LAM(K)/ARG(K)
185    PHIR(K) = ATAN(TA(K))
       SI(K) = SIN(PHIR(K))
       PHIR(K) = PHIR(K)* 57.2957795
       CLSIG(K) = 2. * (ES(K)+EP(K))*SI(K)
       SIG(K) = CLSIG(K)/CL
190    NC(K) = PI*SO(K)*SIG(K)
       C(K) = NC(K)/(NBLAD-2.)
145    BETA(K) = PHIR(K) + ALPHA(K)
C
C   CUTPUT - TABLE 2B
195 C
       WRITE(3,1010)
1010   FCRMAT(//62X,'TABLE 2R'//48X,'1',9X,'2',9X,'3',9X,'4',9X,'5',9X,
       1      '6',9X, '7'/)
200    WRITE(3,1011) (SC(I),I=1,7), (X(I),I=1,7), (LAM(I),I=1,7),
       1      (EP(I),I=1,7), (ES(I),I=1,7),(OIFF(I),I=1,7),
       2      (ARG(I),I=1,7), (TA(I),I=1,7), (PHIR(I),I=1,7),
       3      ,(SI(I),I=1,7),(CLSIG(I),I=1,7), (SIG(I),I=1,7),
       4      (NC(I),I=1,7), (C(I),I=1,7),(ALPHA(I),I=1,7),
       5      (BETA(I), I=1,7)
205 1011 FORMAT(/ 19X,'1  E (STATION DIA - FT)',5X,7(F5.2,5X)/19X,'2  X',
       1      24X,7(F5.2,5X)/ 19X,'3  LAMBOA',19X,7(F5.3,5X)/19X, '4  EP',
       2      23X,7(F5.3,5X)/ 19X,'5,6ES',23X,7(F5.3,5X)/ 19X, '7  ES-EP',
       3      23X,7(F5.3,5X)/ 19X,'8  1 - .5(ES-EP)*LAMBOA',5X,7(F5.3,5X)/
210    4      19X,'9  TAN(PHIR)',16X,7(F5.3,5X)/ 19X,'1U PHIR',21X,7(F5.2
       5      ,5X)/ 19X,'11 SIN(PHIR)',16X, 7(F5.3,5X)/ 19X, '12 CL*SIGMA
       E',17X,7(F5.3,5X)/ 19X,'13 SIGMA',20X, 7(F5.3,5X)/ 19X, '14 N.C.',
       7      21X,7(F5.2,5X)/ 19X,'15 C',24X, 7(F5.3,5X)/ 19X,'16 ALPHA',20X,
       8      7(F5.2,5X)/ 19X,'17 OETA',21X, 7(F5.2,5X)//)
C
215 C   TABLE 2C - STRAIGHTENER CESIGN
C
       GO TO (151,152), OPT1
220 152 DO 155 J = 1,7
       IF(ES(J).LT..5) GO TO 153
```

```
           SC(J) = (2.18 - 1.43*ES(J))/(2.*ES(J)* SIN(ATAN(2./ES(J))))
           GO TO 154
153    SC(J) = 1.5
154    AL2(J) = ATAN(ES(J))* 57.2957795
       THET(J) = AL2(J)/(1. - .26*SQRT(SC(J)))
       NC(J) = PI*SO(J)/SC(J)
155    C(J) = NC(J)/ NELAO

C
C      OUTPUT - TABLE 2C
C
       WRITE(3,1012)
1012   FORMAT(/62X,'TABLE 2C'//48X,'1',9X,'2',9X,'3',9X,'4',9X,'5',9X,
      1 '6',9X,'7'/)
       WRITE(3,1013) (ES(I),I=1,7), (SC(I),I=1,7), (AL2(I),I=1,7),
      1 (THET(I),I=1,7), (NC(I),I=1,7), (C(I),I=1,7)
1013   FORMAT(/33X,'1 ES',9X,7(F5.3,5X)/ 33X,'2 S/C',8X,7(F5.2,5X)/
      1 33X,'3 ALPHA1',5X,7(F5.2,5X)/ 33X,'4 THETA',6X,7(F5.2,5X)
      2 / 33X,'5 N.C.',7X,7(F5.2,5X)/ 33X,'6 C',10X, 7(F5.3,5X)/
      3 /)
       WRITE(3,1008)NBLAO

C
C      TABLE 3 - OFF DESIGN CHARACTERISTICS
C
151    READ(1,1014) (ALPHA(I),I=1,8) ,(CL1(I),I=1,8),(GAMMA(I),I=1,8)
1014   FORMAT(8F10.2)
201    BET = BETA(4)
203    DO 204 I = 1,8
204    BETA(I) = BET
       EPC = EP(4)
       DO 176 L = 1,8
       PHIR(L) = BETA(L) - ALPHA(L)
       PHIR(L) = PHIR(L) * .01745329
       SI(L) = SIN(PHIR(L))
       TA(L) = TAN(PHIR(L))
       CO(L) = 1./TAN(PHIR(L))
       PHIR(L) = PHIR(L)* 57.2957795
       ARG(L) = CL1(L)*SIG(4)*(1. + CC(L)/GAMMA(L))/(2.*SI(L))
       GO TO (161,162), OPT1
161    EP(L) = EPC
       ES(L) = ARG(L) - EP(L)
       GO TO 163
162    ES(L) = ARG(L)
       EF(L) = 0.
163    CIFF(L) = ES(L) - EP(L)
       CLAM(L) = TA(L)/(1.+0.5*CIFF(L)*TA(L))
       KTH(L) = 2.*(CIFF(L))*V*V/(CLAM(L)*2.*VTIP*VTIP*NT)
       GO TO (171,172), OPT1
171    KFK = CLAM(L)*EF(L)/(SIN(ATAN(2./EP(L)))**2 * (EP(L)+ES(L))*
      1 GAMMA(L))
       GO TO 173
172    KPK = CLAM(L)/(  GAMMA(L)*SIN(ATAN(2./ES(L)))**2)
173    NT1(L) = .99 - CLAM(L)/(  SI(L)*SI(L)*(1./GAMMA(L)) + CO(L))
      1 + 1./(55.5/CL1(L) + CO(L)) - KPK
       K1(L) = KTH1(L)*NT1(L)
       KL(L) =K1(L) * CLAM(L)*CLAM(L)
```

```
            B(L) = FI*0*0/4.*(1.-X8*XB)*VTIF*X(L)*CLAM(L)
            HT1(L) = RHO/G*VTIP*VTIP*KTF1(L)
  176   HP(L) = HT1(L)*B(L)/(550.*NT1(L))

    C
    C    OUTPUT - TABLE 3
    C
280         WRITE(3,1015)
  1015  FORMAT(/62X,'TABLE 3'// 48X,'1',9X,'2',9X,'3', 9X,'4',9X, '5', 9X,
       1        '6',9X,'7',9X,'8'/)
285         WRITE(3,1016) (ALPHA(I),I=1,8), (CL1(I),I=1,8), (GAMMA(I),I=1,8),
       1        (PHIR(I),I=1,8), (SI(I),I=1,8), (CO(I),I=1,8),
       2        (TA(I),I=1,8), (ARG(I),I=1,8), (EP(I),I=1,8),
       3        (ES(I),I=1,8), (DIFF(I),I=1,8),(CLAM(I),I=1,8),
       4        (KTH1(I),I=1,8), (NT1(I),I=1,8),(K1(I),I=1,8),
       5        (KL(I),I=1,8), (B(I),I=1,8), (HT1(I),I=1,8),
       6        (HP(I),I=1,8)
  1016  FORMAT(/23X,'1   ALPHA',15X, 8(F5.2,5X)/ 23X, '2   CL',18X,8(F5.2,5X
       1        )/ 23X,'3   GAMMA',15X,8(F5.1,5X)/ 23X,'4   PHIR',16X,8(F5.2,
       2        5X)/23X, '5   SIN(PHIR)',11X,8(F5.4,5X)/ 23X,'6   COT(PHIR)',
       3        11X,8(F5.3,5X)/ 23X,'7   TAN(PHIR)',11X,8(F5.4,5X)/ 23X,
       4        '8   ES + EP',12X,8(F6.4,4X)/ 23X,'9   EP',18X,8(F5.3,5X)/23X,
       5        '10 ES',18X,8(F5.3,5X)/ 23X, '11 ES-EP',14X,8(F6.3,4X)/23X,
       6        '12 LAMBC4',14X, 8(F5.3,5X)/ 23X, '13 KTH', 16X,8(F6.3,4X)/
       7        23X,'14 NT',18X,8(F5.3,5X)/ 23X, '15 K', 18X, 8(F6.3,4X)/
       8        23X,'16 K*LAMCDA*LAMBCA',5X,8(F5.4,5X)/ 23X,'17 FLOW = 0',
       9        12X,8(F5.0,5X)/ 23X,'18 HT',18X,8(F5.2,5X)/ 23X,'19 HP',18X,
       A        8(F5.1,5X)/)
305     GO TO 333
    335 STOP
        END
```

HT =   36.00      Q =  1250.00

NS =    4.614     OS =     1.411

## TABLE 1

| | | | |
|---|---|---|---|
| 1 | 0 FAN DIA. (FT) | = | 4.50 |
| 2 | OB BOSS DIA (FT) | = | 2.25 |
| 3 | N (R.P.M.) | = | 1698. |
| 4 | XB | = | 0.50 |
| 5 | V | = | 104.8 |
| 6 | .5*RHO/G*V*V | = | 13.09 |
| 7 | KTH | = | 3.438 |
| 8 | VTIP | = | 400.0 |
| 9 | V/VTIP | = | 0.262 |
| 10 | LAMBDAB | = | 0.524 |
| 11 | ER | = | 0.901 |
| 12 | CLSIGMA | = | 1.019 |
| 13 | CL | = | 0.635 |
| 14 | SIGMA | = | 1.604 |
| 15 | XBAR | = | 0.750 |
| 16 | LAMBDA BAR | = | 0.349 |
| 17 | EBAR | = | 0.600 |
| 18 | GAMMA*KR/KTH | = | 2.64 |
| 19 | (KRP + KPS)/KTH | = | 0.129 |
| 20 | KRA/KTH | = | 0.040 |
| 21 | NR | = | 0.851 |
| 22 | GAMMA*KS/KTH | = | 0.381 |
| 23 | KS/KTH | = | 0.011 |
| 24 | KD | = | 0.087 |
| 25 | KD/KTH | = | 0.025 |
| 26 | NT | = | 0.814 |

## TABLE 2B

| | | 1 | 2 | 3 | 4 | 5 | 6 | 7 |
|---|---|---|---|---|---|---|---|---|
| 1 | D (STATION DIA - FT) | 2.25 | 2.63 | 3.00 | 3.38 | 3.75 | 4.13 | 4.50 |
| 2 | X | 0.50 | 0.58 | 0.67 | 0.75 | 0.83 | 0.92 | 1.00 |
| 3 | LAMBDA | 0.524 | 0.449 | 0.393 | 0.349 | 0.314 | 0.286 | 0.262 |
| 4 | EP | 0.0 | 0.0 | 0.0 | 0.0 | 0.0 | 0.0 | 0.0 |
| 5,6 | FS | 0.885 | 0.758 | 0.664 | 0.590 | 0.531 | 0.483 | 0.442 |
| 7 | ES-EP | 0.885 | 0.758 | 0.664 | 0.590 | 0.531 | 0.483 | 0.442 |
| 8 | 1 - .5(ES-EP)*LAMBDA | 0.768 | 0.830 | 0.870 | 0.897 | 0.917 | 0.931 | 0.942 |
| 9 | TAN(PHIR) | 0.682 | 0.541 | 0.452 | 0.389 | 0.343 | 0.307 | 0.278 |
| 10 | PHIR | 34.30 | 28.43 | 24.32 | 21.28 | 18.93 | 17.07 | 15.54 |
| 11 | SIN(PHIR) | 0.563 | 0.476 | 0.412 | 0.363 | 0.374 | 0.293 | 0.268 |
| 12 | CL*SIGMA | 0.997 | 0.722 | 0.547 | 0.428 | 0.345 | 0.283 | 0.237 |
| 13 | SIGMA | 0.997 | 0.722 | 0.547 | 0.428 | 0.345 | 0.283 | 0.237 |
| 14 | N.C. | 7.05 | 5.95 | 5.15 | 4.54 | 4.06 | 3.67 | 3.35 |
| 15 | C | 0.587 | 0.496 | 0.429 | 0.378 | 0.338 | 0.306 | 0.279 |
| 16 | ALPHA | 5.50 | 5.50 | 5.50 | 5.50 | 5.50 | 5.50 | 5.50 |
| 17 | BETA | 39.80 | 33.93 | 29.92 | 26.78 | 24.43 | 22.57 | 21.04 |

TABLE 2C

|  | 1 | 2 | 3 | 4 | 5 | 6 | 7 |
|---|---|---|---|---|---|---|---|
| 1 FS | 0.885 | 0.758 | 0.664 | 0.590 | 0.531 | 0.483 | 0.442 |
| 2 S/C | 0.57 | 0.77 | 0.98 | 1.18 | 1.38 | 1.50 | 1.50 |
| 3 ALPHA1 | 41.51 | 37.18 | 33.57 | 30.54 | 27.97 | 25.77 | 23.87 |
| 4 THETA | 51.50 | 48.19 | 45.19 | 42.56 | 40.29 | 37.80 | 35.02 |
| 5 N.C. | 12.51 | 10.68 | 9.65 | 8.98 | 8.51 | 8.64 | 9.42 |
| 6 C | 0.962 | 0.921 | 0.742 | 0.691 | 0.655 | 0.665 | 0.725 |

NUMBER OF BLADES - STATOR = 13.

TABLE 3

|  | 1 | 2 | 3 | 4 | 5 | 6 | 7 | 8 |
|---|---|---|---|---|---|---|---|---|
| 1 ALPHA | -2.50 | 0.0 | 2.50 | 5.00 | 7.50 | 10.00 | 12.50 | 14.50 |
| 2 CL | 0.22 | 0.46 | 0.72 | 0.98 | 1.20 | 1.40 | 1.53 | 1.62 |
| 3 GAMMA | 12.0 | 43.0 | 74.0 | 83.0 | 86.0 | 66.0 | 47.0 | 40.0 |
| 4 PHIR | 24.78 | 26.78 | 24.28 | 21.78 | 19.28 | 16.78 | 14.28 | 12.28 |
| 5 SIN(PHIR) | .4890 | .4505 | .4112 | .3710 | .3301 | .2887 | .2466 | .2127 |
| 6 COT(PHIR) | 1.744 | 1.982 | 2.217 | 2.503 | 2.859 | 3.317 | 3.930 | 4.595 |
| 7 TAN(PHIR) | .5607 | .5046 | .4511 | .3995 | .3498 | .3015 | .2545 | .2176 |
| 8 ES + EP | 0.1106 | 0.2287 | 0.3961 | 0.5825 | 0.8040 | 1.0905 | 1.4392 | 1.8182 |
| 9 EP | 0.0 | 0.0 | 0.0 | 0.0 | 0.0 | 0.0 | 0.0 | 0.0 |
| 10 ES | 0.111 | 0.229 | 0.386 | 0.583 | 0.804 | 1.090 | 1.439 | 1.818 |
| 11 ES-EP | 0.111 | 0.229 | 0.386 | 0.583 | 0.804 | 1.090 | 1.439 | 1.818 |
| 12 LAMBDA | 0.408 | 0.358 | 0.311 | 0.768 | 0.230 | 0.194 | 0.161 | 0.136 |
| 13 KTH | 0.407 | 0.958 | 1.861 | 3.256 | 5.244 | 8.423 | 13.382 | 20.016 |
| 14 NT | 0.772 | 0.900 | 0.012 | 0.902 | 0.888 | 0.859 | 0.817 | 0.780 |
| 15 K | 0.314 | 0.863 | 1.698 | 2.937 | 4.656 | 7.235 | 10.938 | 15.618 |
| 16 K*LAMBDA*LAMBDA | .0522 | .1105 | .1645 | .2116 | .2463 | .2779 | .2847 | .2900 |
| 17 FLOW = 0 | 1946. | 1707. | 1485. | 1281. | 1097. | 927. | 770. | 650. |
| 18 HT | 9.96 | 21.07 | 31.36 | 40.35 | 46.97 | 52.04 | 54.29 | 55.30 |
| 19 HP | 45.7 | 72.7 | 92.8 | 104.1 | 105.5 | 102.1 | 92.9 | 83.8 |

HT =   36.00      Q =   1250.00

NS =   4.614     DS =   1.411

TABLE 1

| | | |
|---|---|---|
| 1 | D FAN DIA. (FT) | = 4.50 |
| 2 | D BOSS DIA. (FT) | = 2.25 |
| 3 | N (R.P.M.) | = 1698. |
| 4 | XB | = 0.50 |
| 5 | V | = 104.8 |
| 6 | .5*RHO/G*V*V | = 13.09 |
| 7 | KTH | = 3.438 |
| 8 | VTIP | = 400.0 |
| 9 | V/VTIP | = 0.262 |
| 10 | LAMBDAB | = 0.524 |
| 11 | EB | = 0.901 |
| 12 | CLSIGMA | = 0.703 |
| 13 | CL | = 0.818 |
| 14 | SIGMA | = 0.859 |
| 15 | XBAR | = 0.750 |
| 16 | LAMBDA BAR | = 0.349 |
| 17 | FBAR | = 0.600 |
| 18 | GAMMA*KR/KTH | = 3.84 |
| 19 | (KRP + KRS)/KTH | = 0.188 |
| 20 | KRA/KTH | = 0.020 |
| 21 | NR | = 0.792 |
| 22 | GAMMA*KP/KTH | = 0.381 |
| 23 | KP/KTH | = 0.010 |
| 24 | KD | = 0.047 |
| 25 | KD/KTH | = 0.025 |
| 26 | NT | = 0.757 |

TABLE 2A

| | 1 | 2 | 3 | 4 | 5 | 6 | 7 |
|---|---|---|---|---|---|---|---|
| 1 D (STATION DIA - FT) | 2.25 | 2.63 | 3.00 | 3.38 | 3.75 | 4.13 | 4.50 |
| 2 X | 0.50 | 0.58 | 0.67 | 0.75 | 0.83 | 0.92 | 1.00 |
| 3 LAMBDA | 0.524 | 0.449 | 0.393 | 0.349 | 0.314 | 0.286 | 0.262 |
| 4 FB | 0.951 | 0.815 | 0.714 | 0.634 | 0.571 | 0.519 | 0.476 |
| 5 ALPHA2 | 43.57 | 39.22 | 35.51 | 32.39 | 29.72 | 27.43 | 25.44 |
| 6 L/C | 1.16 | 1.32 | 1.49 | 1.50 | 1.50 | 1.50 | 1.50 |
| 7 THETA | 56.76 | 53.32 | 50.55 | 46.26 | 42.45 | 39.18 | 36.34 |
| 8 N.C. | 6.07 | 6.23 | 6.33 | 7.07 | 7.85 | 8.64 | 9.42 |

NUMBER OF BLADES - STATOR = 13.

TABLE 2B

| | 1 | 2 | 3 | 4 | 5 | 6 | 7 |
|---|---|---|---|---|---|---|---|
| 1 D (ST/TAN(PHI/2) - FT) | 3.26 | 2.63 | 3.00 | 3.38 | 3.75 | 4.13 | 4.50 |
| 2 X | 0.50 | 0.58 | 0.67 | 0.75 | 0.83 | 0.92 | 1.00 |
| 3 TAN(PHI) | 0.524 | 0.449 | 0.393 | 0.349 | 0.314 | 0.286 | 0.262 |
| 4 FDS | 0.951 | 0.815 | 0.714 | 0.634 | 0.571 | 0.519 | 0.476 |
| 5 CS | 0.0 | 0.0 | 0.0 | 0.0 | 0.0 | 0.0 | 0.0 |
| 6 FS-FD | -.351 | -.915 | -.714 | -.634 | -.571 | -.519 | -.476 |
| 7 1-FS(FS-FD)*LAMBDA | 1.246 | 1.183 | 1.140 | 1.111 | 1.090 | 1.074 | 1.062 |
| 8 TAN(PHI/2) | 0.416 | 0.345 | 0.345 | 0.314 | 0.248 | 0.266 | 0.247 |
| 9 DHL | 22.76 | 26.79 | 19.02 | 17.46 | 16.09 | 14.90 | 13.85 |
| 10 SIN(PHI/2) | 0.347 | 0.355 | 0.326 | 0.300 | 0.277 | 0.257 | 0.239 |
| 11 CL*SIGMA | 0.775 | 0.574 | 0.465 | 0.381 | 0.316 | 0.267 | 0.228 |
| 12 SIGMA | 0.734 | 0.570 | 0.465 | 0.381 | 0.316 | 0.267 | 0.228 |
| 13 N.C. | 5.20 | 4.77 | 4.38 | 4.03 | 3.73 | 3.46 | 3.22 |
| 14 ALPHA | 0.434 | 0.398 | 0.365 | 0.336 | 0.311 | 0.288 | 0.268 |
| 15 BETA | 5.50 | 5.50 | 5.50 | 5.50 | 5.50 | 5.50 | 5.50 |
| | 25.72 | 24.20 | 24.62 | 22.96 | 21.59 | 20.40 | 19.35 |

TABLE 3

| | 1 | 2 | 3 | 4 | 5 | 6 | 7 | 8 |
|---|---|---|---|---|---|---|---|---|
| 1 ALPHA | -2.50 | 0.0 | 2.50 | 5.00 | 7.50 | 10.00 | 12.50 | 14.50 |
| 2 CL | 0.22 | 0.44 | 0.72 | 0.98 | 1.20 | 1.40 | 1.53 | 1.62 |
| 3 GAMMA | 19.0 | 43.0 | 74.0 | 84.0 | 86.0 | 66.0 | 47.0 | 40.0 |
| 4 PHI | 25.44 | 22.06 | 20.46 | 17.96 | 15.46 | 12.96 | 10.46 | 8.46 |
| 5 SIN(PHI) | .4295 | .3605 | .3495 | .7693 | .2665 | .2242 | .1915 | .1471 |
| 6 COT(PHI) | 2.171 | 2.341 | 2.641 | 3.086 | 3.616 | 4.346 | 5.418 | 6.726 |
| 7 TAN(PHI) | .4761 | .4236 | .3730 | .3241 | .2765 | .2301 | .1846 | .1487 |
| 8 CS + CD | 0.144 | 0.367 | 0.4062 | 0.6272 | 0.4927 | 1.2662 | 1.7888 | 2.4482 |
| 9 CS | 0.434 | 0.434 | 0.634 | 0.634 | 0.634 | 0.634 | 0.634 | 0.634 |
| 10 CS-CD | -.526 | -.438 | -.228 | -.007 | 0.258 | 0.632 | 1.155 | 1.814 |
| 11 LAMBDA | -1.164 | -1.032 | -0.962 | -0.641 | -0.376 | -0.007 | 0.520 | 1.180 |
| 12 XTH | 0.246 | 0.407 | 0.633 | 0.271 | 0.219 | 0.173 | 0.132 | 0.103 |
| 13 ST | 0.464 | 0.973 | 1.327 | 3.449 | 6.121 | 11.004 | 20.315 | 35.820 |
| 14 ... | 0.162 | 0.738 | 0.879 | 0.868 | 0.852 | 0.809 | 0.749 | 0.690 |
| 15 ...LAMBDA | 0.232 | 1.210 | 1.607 | 3.012 | 5.202 | 8.907 | 15.209 | 24.709 |
| 16 ... | 2340. | 1940. | 1591. | 1294. | 1044. | 824. | 630. | 489. |
| 17 FLOW = 0 | 7.47 | 23.25 | 34.06 | 42.77 | 47.48 | 50.61 | 50.60 | 49.53 |
| 18 HT | 48.5 | 97.1 | 112.0 | 114.5 | 106.0 | 93.6 | 77.4 | 63.9 |

# APPENDIX C
## CENTRIFUGAL FAN WEIGHT ESTIMATE

NOMENCLATURE

$b_i$      – Inside blade height, ft

$b_O$      – Outside blade height, ft

$d_i$      – Inside fan diameter, ft

$d_O$      – Outside fan diameter, ft

$d_H$      – Hub diameter, ft

$h_H$      – Hub height, ft

$t_1$      – Base plate thickness, ft

$t_2$      – Upper shroud thickness, ft

$t_{3avg}$      – Average blade thickness, ft

$W_1$      – Base plate weight, lb

$W_2$      – Upper shroud weight, lb

$W_3$      – Blade weight, lb

$W_4$      – Hub weight, lb

$W_{CF}$      – Centrifugal fan weight, lb

$z$      – Number of blades

$\beta_i$      – Inlet blade angle, degrees

$\beta_O$      – Outlet blade angle, degrees

$\rho$      – Fan material density, $lb_m/ft^3$

1      – Base plate

2      – Upper shroud

3      – Fan blades

4      – Hub.

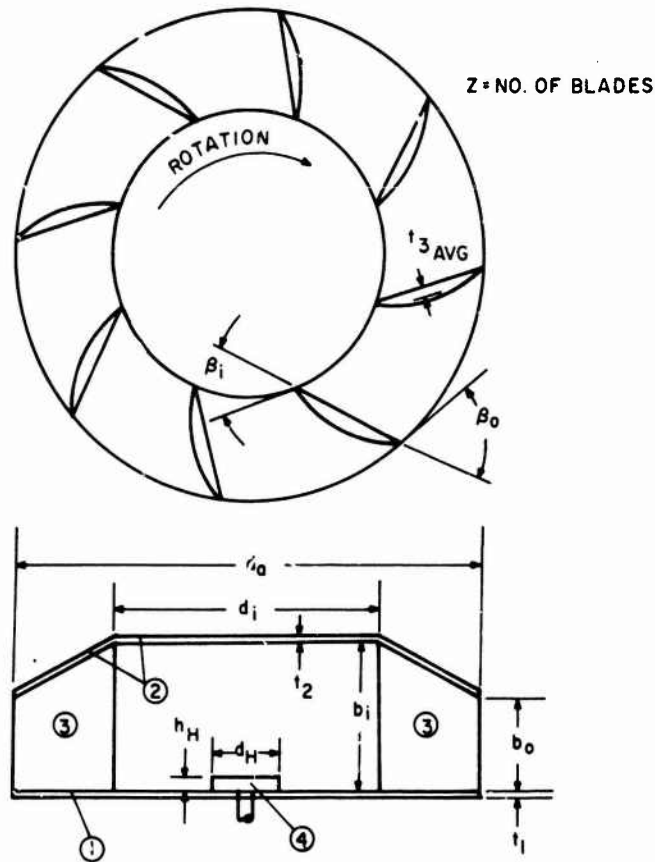The centrifugal fan weight is composed of four main parts as shown in figure 1-C.



Figure 1-C
Centrifugal Fan Basic Geometry

The base plate weight:

$$W_1 = \rho t_1 \frac{\pi d_o^2}{4} \; .$$

(1)

The upper shroud weight:

$$W_2 = \pi \rho t_2 \left( \frac{d_i + d_o}{4} \right) \left[ \left( \frac{d_o - d_i}{2} \right)^2 + (b_i - b_o)^2 \right]^{1/2} \; .$$

(2)

The blade weight:

$$W_3 = \frac{z\rho t_3}{\cos\left(90° - \frac{\beta_i + \beta_0}{2}\right)} \cdot \left(\frac{d_0 - d_i}{2}\right)\left(\frac{b_0 + b_i}{2}\right) \cdot \quad (3)$$

The hub weight:

$$W_4 = \rho h_H \frac{\pi d_H^2}{4} \cdot \quad (4)$$

The basic centrifugal fan weight is obtained by adding equations (1) through (4). Thus,

$$W_{CF} = W_1 + W_2 + W_3 + W_4 \cdot \quad (5)$$

# INITIAL DISTRIBUTION

| Copies | | Copies | |
|---|---|---|---|
| 1 | OASN (Cdr J. T. Parker) | 1 | NASA Hdqtrs |
| 1 | ONR (Code 415) | 1 | U. S. Naval Academy (J. F. Sladky, Jr.) |
| 4 | ARPA* | | |
| 1 | U. S. Marine Corps (RD&S) | 2 | DDC |
| 1 | U. S. Marine Corps Dev. & Ed. Comm. | 1 | Aerojet General Corp. (Mr. Shenfil) |
| 5 | NAVSHIPS | 1 | Aerospace Corp. (Mr. R. T. Scott) |
| | 1 (SHIPS 031) | | |
| | 1 (SHIPS 03Z2) | 1 | Bell Aerospace Co. (Mr. Hite) |
| | 1 (SHIPS 03421) | | |
| | 2 (SHIPS 2052) | 1 | Boeing Co. (Mr. Miller) |
| 1 | SESPO (PM 17) | | |
| 1 | NAVAIR (Code 303B) | 1 | Booz-Allen Applied Research, Inc. (Mr. Willard) |
| 1 | NAVSEC (SEC 6101F) | | |
| 1 | NELC (D. Forbes) | 1 | Developmental Sciences, Inc. (Dr. Seemann) |
| 1 | U. S. Army, MERDC (M&BD) (John Sargent) | | |
| | | 1 | Goodyear Aerospace Corp. (Mr. Cross) |
| 1 | U. S. Army, Res. Office | | |
| 1 | U. S. Air Force, FDL (FEM) (Dr. K. H. Digges) | 1 | Hamilton Standard (Mr. Deabler) |
| 1 | U. S. Coast Guard Hdqtrs (R&D) | 1 | Oceanics, Inc. (Mr. Kaplan) |
| 1 | DOT, High Speed Ground Transportation (Mr. A. F. Lampros) | 1 | Grumman Aerospace Corp. (Mr. Munz) |

---

*Addressee.

INITIAL DISTRIBUTION (Cont)

Copies

   1     Johns Hopkins Univ.
           Applied Physics Lab.
           (Mr. Paddison)

   1     USA, Cold Regions R&D Lab.
           (Dr. K. F. Sterrett)

   1     Arctic Inst. of North America
           (Mr. Robert Faylor)

CENTER DISTRIBUTION

| Copies | Code |
|---|---|
| 1 | (11) (W. Ellsworth) |
| 20 | (113) (J. U. Kordenbrock) |
| 1 | (115) (Dr. D. A. Jewell) |
| 1 | (118) (M. W. Brown) |
| 1 | (1572) (Mrs. M. Ochi) |
| 1 | (161) (R. L. Schaeffer) |
| 3 | (1735) (R. G. Allen) |
| 1 | (1748) (O. Hackett) |
| 1 | (2721) (R. K. Muench) |
| 20 | (2721) (J. G. Purnell) |
| 1 | (2803) (J. J. Kelly) |
| 30 | (5614) |
| 1 | (5641) |
| 1 | (5642) |
| 1 | (5811) |
| 1 | (9401) (Capt Boyd) |

## DOCUMENT CONTROL DATA - R & D

*(Security classification of title, body of abstract and indexing annotation must be entered when the overall report is classified)*

| 1. ORIGINATING ACTIVITY (Corporate author) | 2a. REPORT SECURITY CLASSIFICATION |
|---|---|
| Naval Ship Research and Development Center Annapolis, Maryland 21402 | Unclassified |
| | 2b. GROUP |

**3. REPORT TITLE**

Prediction of Axial and Centrifugal Fan Characteristics for Large Surface Effect Vehicles

**4. DESCRIPTIVE NOTES** *(Type of report and inclusive dates)*

Research and Development

**5. AUTHOR(S)** *(First name, middle initial, last name)*

J. G. Purnell

| 6. REPORT DATE | 7a. TOTAL NO. OF PAGES | 7b. NO. OF REFS |
|---|---|---|
| July 1973 | 86 | 16 |

| 8a. CONTRACT OR GRANT NO. | 9a. ORIGINATOR'S REPORT NUMBER(S) |
|---|---|
| b. PROJECT NO. | |
| | 3943 |
| c. | 9b. OTHER REPORT NO(S) *(Any other numbers that may be assigned this report)* |
| Work Unit 1-1130-300-05 d. | 27-404 |

**10. DISTRIBUTION STATEMENT** Distribution limited to U. S. Government agencies only; Test and Evaluation; July 1973. Other requests for this document must be referred to Commander, Naval Ship Research and Development Center (Code 11), Bethesda, Maryland 20034.

| 11. SUPPLEMENTARY NOTES | 12. SPONSORING MILITARY ACTIVITY |
|---|---|
| | ARPA |

**13. ABSTRACT**

Two digital computer programs have been formulated for predicting performance characteristics of centrifugal and axial fans which may be used to provide lift air for large surface effect vehicles. Pressure rise and flow characteristics of forwardly curved, radial, and backwardly curved centrifugal fans can be evaluated. Axial fans having either inlet flow prerotators or exit flow straighteners can also be handled in the program. Sample results are presented to illustrate the method of calculation and the nature of the results.

(Author)

**DD** FORM 1 NOV 65 **1473** (PAGE 1)

S/N 0101-807-6801

| 14 KEY WORDS | LINK A | | LINK B | | LINK C | |
|---|---|---|---|---|---|---|
| | ROLE | WT | ROLE | WT | ROLE | WT |
| Axial fans | | | | | | |
| Centrifugal fans | | | | | | |
| Fan characteristics | | | | | | |
| Lift fans | | | | | | |
| Fan performance | | | | | | |